THEORY OF CONDENSED MATTER AND NEW MATERIALS

CONTENTS

THEORY OF CONDENSED MATTER AND NEW MATERIALS

INTRODUCTION

In the years 2011-2012 investigations within the theme "Theory of Condensed Matter and New Materials" were continued in the framework of the following projects:

- Physical properties of complex materials and nanostructures;
- Mathematical problems of many-particle systems.

The first project followed the modern trends in condensed matter physics and covered two important topics. Complex materials under study include high-temperature superconductors, magnetic systems, layered structures etc. Theoretical studies in this field are based on multiparticle models of solids taking into consideration strong electron correlations, electron-lattice, and spin interactions to describe spectra of quasiparticle excitations, phase transitions and kinetic phenomena in solids. In the theory of superconductivity, one considers nonstandard mechanisms of pairing in metal-oxides, the influence of the inter-site Coulomb repulsion and electron-phonon interaction on the superconducting transition temperature, intrinsic Josephson junctions in high temperature superconductors, as well as a problem of instability of the Nagaoka state. The contributions by A.A. Vladimirov, D. Ihle, N.M. Plakida and by E.A. Kochetov with co-authors show new achievements in these studies within the $t - J$ model. In the contribution by Yu.M. Shukrinov, I.R. Rahmonov and M.A. Gaafar the plasma frequency of a stack of coupled Josephson junctions irradiated with electromagnetic waves was calculated. It was shown that the nonequilibrium situation in the thin superconducting layers of high temperature superconductors plays an important role in the variety of novel phenomena in the system of Josephson junctions.

In the theory of nanostructures, there were examined magnetic and electronic properties of carbon-based systems, ferromagnetic or antiferromagnetic type of ordering and the role of defects in this type of materials, mechanisms of phase transitions caused by charge, orbital, and magnetic ordering in magnetic thin films and nanomaterials, the electronic spectrum of carbon materials within the field-theory model adapted to account for nontrivial geometry of these nanostructures, as well as electron and heat transport in electrode-molecule-electrode devices. The contribution by A.A. Dzhioev and D.S. Kosov is devoted to studies of the electron transport through nanoscale quantum systems. The authors developed an original theoretical approach which is based on a Lindblad master equation for the density matrix of an open quantum system and a superoperator formalism.

New interesting results were obtained in the theory of small-angle neutron scattering from multiphase fractal systems. These studies are performed in collaboration with the Frank Laboratory of Neutron Physics, JINR. In the contribution by A.Yu. Cherny, E.M. Anitas, V.A. Osipov and A.I. Kuklin prospects for investigating deterministic fractals were discussed and a possibility for extracting additional information from small-angle scattering data was shown.

Among other interesting studies one should mention the processes of multifragmentation, clusterization in phase transitions and the influence of surface effects on the properties of clusters in equilibrium and nonequilibrium media with strong correlations such as liquids and nuclear matter. In the theory of finite quantum systems, low-dimensional states of matter obtained in modern experiments, in particular, properties of quasiparticles in mesoscopic systems and the Bose-Einstein condensation in atomic traps were studied.

The second project dealt with modern problems of statistical mechanics. Many-body systems of equilibrium and non-equilibrium statistical physics related to stochastic models of interacting particles were investigated with an emphasis on asymptotic scaling laws associated with large scale universal behaviour of a wide class of systems, exact derivation of these laws, investigation of the mathematical mechanisms governing the models and search for links between them. The studies were carried out with modern methods of the enumerative combinatorics, theories of integrable systems, determinant processes, random matrices and conformal field theory. Special attention to studies within the well-known sandpile and random walk models was paid. There were considered various integrable models of two-dimensional lattice spin systems with continuous values of spins. New inequalities in equilibrium statistical mechanics were considered in the contribution by J.G. Brankov and N.S. Tonchev. In the contribution by V.S. Poghosyan and V.B. Priezzhev the exact critical exponent for two-dimensional k-leg watermelon was derived. S.S. Poghoyan, A.M. Povolotsky and V.B. Priezzhev presented the universal exit probabilities in the totally asymmetric simple exclusion process.

V.A. Osipov, J. Brankov

SUPEROPERATOR REPRESENTATION OF LINDBLAD MASTER EQUATION FOR ELECTRON TRANSPORT PROBLEM

A.A. Dzhioev[1] and D. S. Kosov[2]

[1] Bogoliubov Laboratory of Theoretical Physics, Joint Institute for Nuclear Research, RU-141980 Dubna, Russia

[2] School of Engineering and Physical Sciences, James Cook University, Townsville, QLD, 4811, Australia

Study of the electron transport through nanoscale quantum systems (molecules, quantum dots, etc.) remains one of the most active areas of contemporary condensed matter physics. So far, much of the theoretical and computational studies have been based on the Keldysh nonequilibrium Green functions, but the understanding of fundamental mechanisms of transport in nanoscale systems also requires the development of new theoretical approaches to nonequilibrium interacting many-body quantum systems.

In this contribution, we give an account of our recent efforts [1-4] to develop an alternative theoretical approach to the problem of electron transport through interacting systems. Our approach is based on two main ingredients: a Lindblad master equation for the density matrix of an open quantum system and a superoperator formalism which enable us to convert this master equation into a non-Hermitian Shrödinger-like equation in the Liouville space.

We consider the paradigmatic model of the electron transport theory: a quantum system (central region) coupled to two noninteracting electrodes, left (L) and right (R). The central region can contain electron-electron or electron-vibration interactions. As usual, we assume that the electrode - central region coupling has a tunneling form. The system is brought into a nonequilibrium state by applying an external voltage, which relatively shifts chemical potential of the electrodes and supports electron transport (current) through the central region.

To derive the Lindblad equation we introduce an embedded quantum system, which consists of the central region and the finite buffer zones between the central region and the environments (see Fig. 1). Projecting out the environment degrees of freedom from the Liouville equation for the total density matrix, we obtain the master equation for the reduced density matrix of the embedded system

$$i\frac{\partial \rho(t)}{\partial t} = [H, \rho(t)] + i\Pi\rho(t). \tag{1}$$

Here, $H(a^\dagger, a)$ is the Hamiltonian of the embedded system in the second-quantized form and $\Pi(a^\dagger, a)$ is the non-Hermitian dissipator which represents the influence of the environment on the embedded system. The dissipator depends on the temperature $T_{L,R}$ and the chemical potential $\mu_{L,R}$ in the left and right electrodes.

The Lindblad master equation (1) describes the time evolution of the open quantum system preserving hermiticity, trace 1, and positivity of the nonequilibrium density matrix $\rho(t)$. We have demonstrated that this embedding procedure makes the master equation exact in the steady-state regime, provided the buffer zones are large enough to

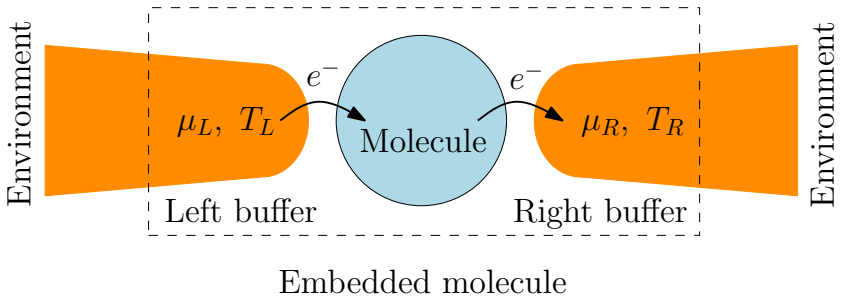

Figure 1: Schematic illustration of molecule embedding. The electrodes are divided into macroscopic "environment" and buffer zone. Each buffer zone contains a finite number of discrete single-particle levels.

cure the deficiencies of the Born-Markov approximation for treating the interface between the environment and the buffer zones [3].

To convert the Lindblad master equation to a form suitable for many-body calculations, it is convenient to represent the density matrix as a vector $|\rho\rangle$ in the Liouville space and other operators as superoperators. For this purpose, in [1,2,4] we have introduced non-tilde, $\hat{a}^\dagger(\hat{a})$, and tilde, $\widetilde{a}^\dagger(\widetilde{a})$, creation (annihilation) superoperators which obey the same commutation rules as ordinary particle operators $a^\dagger,\ a$. Non-tilde superoperators represent particle operators acting on the density matrix from the left, while tilde superoperators represent operators acting from the right. With the help of superoperators we can rewrite the Lindblad master equation as the Srödinger-like equation for $|\rho(t)\rangle$

$$i\frac{\partial}{\partial t}\,|\rho(t)\rangle = L\,|\rho(t)\rangle, \tag{2}$$

where $L = L(\hat{a}^\dagger, \widetilde{a}^\dagger, \hat{a}, \widetilde{a})$ is the non-Hermitian superoperator (Liouvillian) which depends on both non-tilde and tilde superoperators. The density matrix is normalized according to $\langle I|\rho(t)\rangle = 1$. Here, $\langle I|$ is the left zero-eigenvalue eigenstate of the Liouvillian (that is, $\langle I|\,L = 0$), which corresponds to the unit operator I.

For the electron transport problem we are interested in the nonequilibrium asymptotic ($t \to \infty$) steady-state, when $|\rho(t)\rangle$ does not depend on time. Therefore, the steady-state solution of Eq. (2) is the right zero-eigenvalue eigenstate of the Liouvillian

$$L\,|\rho_\infty\rangle = 0. \tag{3}$$

Once the solution of this equation is found, the steady state current through the central region can be computed as the following matrix element:

$$J = \langle I|\hat{J}|\rho_\infty\rangle, \tag{4}$$

where $\hat{J}$ is the current superoperator.

In [2,4], the nonequilibrium many-body perturbation theory to solve Eq. (3) was developed. For this purpose, we first determine the unperturbed state. Using the Wick theorem we rewrite the Liouvillian as

$$L = L_0 + \lambda L'. \tag{5}$$

Here, L_0 is a mean-field (quadratic) part and L' contains interaction terms which stem from the central region Hamiltonian. In [1], we have shown that using the equation of motion method we can diagonalize L_0 in terms of nonequilibrium quasiparticle creation and annihilation superoperators

$$L_0 = \sum_n (\Omega_n \hat{c}_n^\dagger \hat{c}_n - \Omega_n^* \widetilde{c}_n^\dagger \widetilde{c}_n). \tag{6}$$

These superoperators are connected to $\hat{a}^\dagger$, $\hat{a}$, $\widetilde{a}^\dagger$, $\widetilde{a}$ by canonical (but not unitary) transformations. This means that although $\hat{c}_n^\dagger$, $\hat{c}_n$ ($\widetilde{c}_n^\dagger$, $\widetilde{c}_n$) are not Hermitian conjugate to each other, they obey the fermionic anticommuation relations. We define the unperturbed (mean-field) density matrix, $|\rho_\infty^{(0)}\rangle$, as a vacuum state for $\hat{c}_n$ and $\widetilde{c}_n$ superoperators, i.e., $L_0 |\rho_\infty^{(0)}\rangle = 0$. Note that by the construction of $\hat{c}_n^\dagger$ and $\widetilde{c}_n^\dagger$, $\langle I|$ is a vacuum state for them.

Expanding the exact density matrix in powers of λ and demanding Eq. (3) to be fulfilled we find the recurrent relation for the pth-order correction to the mean-filed density matrix

$$L_0 |\rho_\infty^{(p)}\rangle = -L' |\rho_\infty^{(p-1)}\rangle. \tag{7}$$

This yields the formal solution for the exact steady-state density matrix ($\lambda = 1$)

$$|\rho_\infty\rangle = \sum_{p=0} |\rho_\infty^{(p)}\rangle = \left(1 + L_0^{-1} L'\right) |\rho_\infty^{(0)}\rangle \tag{8}$$

as well as the perturbation expansion for the current

$$J = \sum_{p=0} \langle I|\hat{J}|\rho_\infty^{(p)}\rangle = \sum_{p=0} J^{(p)}. \tag{9}$$

In Fig. 2, we demonstrate the results of perturbation calculations [2] for the current through the Anderson impurity model. As it follows from our calculations, the second-order correction $J^{(2)}$ to the mean-field current is most pronounced when the impurity is half occupied. Moreover, we observe the increase of $J^{(2)}$ with increasing the external voltage. This means that the nonequilibrium enhances the role of electronic correlations.

For the system with electron-vibration coupling the perturbation theory was developed in [4]. Our further research will be focused on the development and application of nonperturbative methods, such as configuration-interaction and coupled-cluster methods, to the electron transport problem.

1. A.A. Dzhioev, D.S. Kosov, J. Chem. Phys. **134** (2011) 044121-12.

2. A.A. Dzhioev, D.S. Kosov, J. Chem. Phys. **134** (2011) 154107-7.

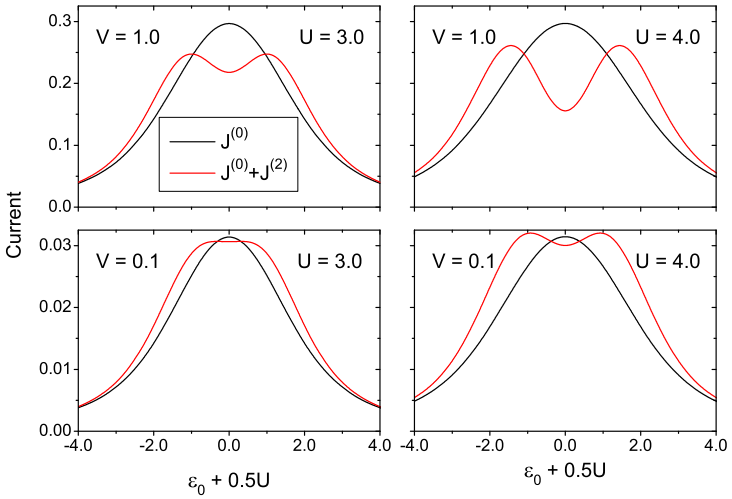

Figure 2: Current through the Anderson impurity model as a function of the central cite energy, ε_0, at external voltages $V = 1.0$ and $V = 0.1$ for different values of the Coulomb interaction energy U (all quantities are given in relative units).

3. A.A. Dzhioev, D.S. Kosov, J. Chem. Phys. **135** (2011) 174111-7.

4. A.A. Dzhioev, D.S. Kosov, J. Phys: Condens. Matter **24** (2012) 225304-12.

We see that second order correction to the mean-field current is most pronounced when the impurity is half occupied.

Effective approach to the Nagaoka regime of the two dimensional t–J model

O. P. Sushkov

June 9, 2013

As is known, at half filling, the infinite–U Hubbard model (or equivalently, the $t-J$ model at $J=0$) has antiferromagnetic (AF) ground state. However, in 1965 Nagaoka proved a theorem[1] which states that when exactly one hole is introduced, the ground state becomes ferromagnetic (FM). In the infinite–U limit the ground state of the half filled Hubbard model is macroscopically degenerate. When a single hole is introduced, this degeneracy is lifted since it is energetically favorable for the hole to move in a background of fully aligned spins.

The Nagaoka theorem is one of very few rigorous results concerning strongly correlated electron systems. However, it does not say anything about the case of a finite density of holes as well as finite AF interaction. The issue of a character of the leading instability of the Nagaoka state with respect to switching on the AF exchange term or finite density of holes attracts much interest.

The aim of the present paper [2] is to identify the leading instability of the Nagaoka state. To this end, we first discuss the recently proposed full Ising version [3] of the $t-J$ model of strongly correlated electrons. While the standard $t-J$ model can be considered as a hole doped quantum Heisenberg spin model, its full Ising version appears as a hole doped classical Ising spin model. We then show that the t–J model and its full Ising version give the same physical picture of the Nagaoka regime for $J/t \ll 1$.

When compared to the standard t–J or t–J_z models, the doped Ising model allows for a numerical analysis on much larger clusters by means of classical Monte Carlo simulations. It also allows for a simple analytical treatment in the physically relevant limit of a small density of doped holes, $\delta \ll 1$. Taking the advantage of those facts, we can study the low doping regime of the t–J model for $J/t \ll 1$ in a controlled and reliable way.

Several variational wave functions were suggested in order to yield bounds for the Nagaoka stability region in the $\delta - J$ plane (See [4] and references therein). Most of those estimates were based on the belief that the transition from Nagaoka state is continuous at $T=0$. In other words, it was assumed that the leading instability of Nagaoka's state is a single spin flip.

Our results provide, however, a strong evidence that the leading instability of the FM Nagaoka state is a phase separation rather than a single spin flip. They suggest that Nagaoka state breaks down through a discontinuous quantum phase transition by forming an FM bubble. The transition between Nagaoka state and this "bubble" state is the first

order one, including a jump in the total spin. Thus, this transition cannot be captured by a single spin flip transition. This observation fully agrees with a conjecture discussed earlier within the isotropic $t-J$ model in the semiclassical (large spin) approximation[5].

Numerically, we show that this transition occurs at a critical hole concentration $\delta_c = 0.44(J/t)^{0.53}$. For $\delta > \delta_c$, the whole system is in a fully polarized FM state. Analytical calculation valid for $\delta \ll 1$ yields $\delta_c = \sqrt{J/2\pi t}$ which is in good agreement with the numerical result.

[1] Y. Nagaoka, Solid State Commun. **3**, 409 (1965); Phys. Rev. **147**, 392 (1966).

[2] M.M. Maska, M. Mierzejewski, E.A. Kochetov, L. Vidmar, J. Bonca, O.P. Sushkov, Phys.Rev. B **85**, 245113 (2012).

[3] M. M. Maśka, M. Mierzejewski. A. Ferraz, and E. A. Kochetov, J. Phys. **C11**, 115135 (2009).

[4] T. Hanish, G.S. Uhrig and E. Müller-Hartmann, Phys.Rev. B **56**, 13960 (1997).

[5] E. Eisenberg, R. Berkovits, David A. Huse, and B. L. Altshuler, Phys. Rev. B **65**, 134437 (2002).

NEW INEQUALITIES IN EQUILIBRIUM STATISTICAL MECHANICS

J. G. Brankov[a,b] and N. S. Tonchev[c]
[a] Joint Institute for Nuclear Research, 141980 Dubna, Russia
[b] Institute of Mechanics, Bulgarian Academy of Sciences, 1113 Sofia, Bulgaria
[c] Institute of Solid State Physics, Bulgarian Academy of Sciences, 1784 Sofia, Bulgaria

1. Bounds on the quadratic fluctuations

A number of important results on the role of critical fluctuations in systems with broken symmetries have been obtained in the past by using famous inequalities due to Bogoliubov, Mermin-Wagner, Griffits, among others, see, e.g. [1, 2, 3, 4]. A remarkable property of this approach is that the results obtained are exact and cannot be inferred from any perturbation theory. The benefits of having exact statements about systems are difficult to overestimate. A survey of inequalities used to solve problems arising in the Approximating Hamiltonian Method, along with their generalizations, is given in our work [5].

The infinite sets of generalized inequalities obtained in [5] provide upper bounds on the difference between the quadratic fluctuations of intensive observables of a N-particle system and the corresponding Bogoliubov - Duhamel inner product. Such bounds are used, e.g., in the majorization technique developed by Bogoliubov Jr. for the needs of the Approximating Hamiltonian method [6]. The results are illustrated by two types of exactly solvable model systems: one with bounded separable attraction and the other containing interaction of a boson field with matter.

In the first case, we assume that the Hamiltonian $\mathcal{H}_\Lambda$ of the system in a finite region of space Λ is a self-adjoint, trace-class operator which generates the Gibbs semi-group $\{\exp(-\beta\mathcal{H}_\Lambda)\}_{\beta\geq 0}$. Let the operators A, $B, \ldots$, belong to the algebra of bounded observables for which the Bogoliubov - Duhamel inner product $(A;B)$ is well defined:

$$(A;B)_{\mathcal{H}} \equiv (Z[\mathcal{H}])^{-1} \int_0^1 \mathrm{d}\tau \, \mathrm{Tr}\left[\mathrm{e}^{-\beta(1-\tau)\mathcal{H}} A^\dagger \mathrm{e}^{-\beta\tau\mathcal{H}} B\right]. \tag{1}$$

Further we assume that the Hamiltonian $\mathcal{H}$ has a discrete, non-degenerate spectrum only, $\{E_n, n = 1, 2, 3 \ldots\}$ and denote by $|n\rangle$ the corresponding eigenfunctions, i.e., $\mathcal{H}|n\rangle = E_n|n\rangle$, $n = 1, 2, 3 \ldots$. By $A_{mn} = \langle m|A|n\rangle$ we denote the corresponding matrix element of an operator A. Then, the spectral representation of the Bogoliubov - Duhamel inner (1) can be written as

$$(A;B)_{\mathcal{H}} = (Z_\Lambda[\mathcal{H}])^{-1} {\sum_{m,n}}' A^*_{mn} B_{mn} \frac{e^{-\beta E_m} - e^{-\beta E_n}}{\beta(E_n - E_m)} + (Z_\Lambda[\mathcal{H}])^{-1} \sum_n \mathrm{e}^{-\beta E_n} A^*_{nn} B_{nn}, \tag{2}$$

where the prime in the double sum means that the term with $n = m$ is excluded.

Our aim is to majorize the quadratic fluctuations

$$\langle \delta A^\dagger \delta A\rangle = \langle A^\dagger A\rangle_{\mathcal{H}} - |\langle A\rangle_{\mathcal{H}}|^2 \tag{3}$$

by terms proportional to some power of the inner product

$$(\delta A;\delta A) = (A;A) - |\langle A\rangle|^2$$
$$= Z_\Lambda^{-1}\sum_{m,n}{}'|A_{mn}|^2\frac{\mathrm{e}^{-\beta E_m}-\mathrm{e}^{-\beta E_n}}{\beta(E_n-E_m)} + (Z_\Lambda[\mathcal{H}])^{-1}\sum_n \mathrm{e}^{-\beta E_n}|A_{nn}|^2 - |\langle A\rangle|^2. \qquad (4)$$

Fot the symmetrized form of (3) we obtain

$$\frac{1}{2}\langle A^\dagger A + AA^\dagger\rangle - (A;A)$$
$$= Z^{-1}\sum_{m,n}{}'|A_{mn}|^2\left\{\frac{1}{2}(\mathrm{e}^{-\beta E_n}+\mathrm{e}^{-\beta E_m}) - \frac{\mathrm{e}^{-\beta E_m}-\mathrm{e}^{-\beta E_n}}{\beta(E_n-E_m)}\right\}, \qquad (5)$$

which, by using the identity

$$\mathrm{e}^{-\beta E_m}+\mathrm{e}^{-\beta E_n} = (\mathrm{e}^{-\beta E_n}-\mathrm{e}^{-\beta E_m})\coth\frac{\beta(E_m-E_n)}{2} \qquad (6)$$

can be expressed as:

$$\frac{1}{2}\langle A^\dagger A + AA^\dagger\rangle - (A;A) = Z^{-1}\sum_{m,n}{}'|A_{mn}|^2\frac{\mathrm{e}^{-\beta E_m}-\mathrm{e}^{-\beta E_n}}{\beta(E_n-E_m)}(X_{mn}\coth X_{mn}-1), \qquad (7)$$

where $X_{mn} = \beta(E_m-E_n)/2$.

Different choices of the upper bound on the right-hand side of (7) generate different inequalities. Thus, the inequality of Brooks Harris [7],

$$(A;A) \le \frac{1}{2}\langle AA^+ + A^+A\rangle \le (A;A) + \frac{\beta}{12}\langle[[A^+,\mathcal{H}],A]\rangle. \qquad (8)$$

is obtained by setting $1 \le x\coth x \le 1 + x^2/3$.

On the other hand, if one uses another elementary inequality, $1 \le x\coth x \le 1+|x|$, and subsequently applies the Hölder inequality, one obtains the result due to Ginibre [8]:

$$(A;A) \le \frac{1}{2}\langle AA^+ + A^+A\rangle \le (A;A) + \frac{1}{2}\{(A;A)\beta\langle[[A^+,\mathcal{H}],A]\rangle\}^{\frac{1}{2}}. \qquad (9)$$

A different choice of the parameters in the Hölder inequality, followed by the implementation of the upper bound

$$|e^{-\beta E_l} - e^{-\beta E_m}| < |e^{-\beta E_l} + e^{-\beta E_m}|, \qquad (10)$$

generates a symmetric version of the inequality due to Bogoliubov, Jr. [6]:

$$\frac{1}{2}\langle AA^+ + A^+A\rangle \le (A;A) + \frac{1}{2}[(A;A)\beta]^{2/3}\{\langle[A^+,\mathcal{H}][\mathcal{H},A] + [\mathcal{H},A][A^+,\mathcal{H}]\rangle\}^{1/3}, \qquad (11)$$

To derive generalizations of the known inequalities involving the Bogoliubov - Duhamel inner product, we define a set of new functionals in terms of their spectral representations:

$$F_{2n}(J;J) \equiv Z^{-1}\sum_{ml}|J_{ml}|^2|e^{-\beta E_l}-e^{-\beta E_m}|(\beta|E_m-E_l|)^{2n-1}$$
$$=\beta^{2n}(R_n;R_n)=\beta^{2n-1}\langle[R_n^+R_{n-1}-R_{n-1}R_n^+]\rangle,\quad n=0,1,2,3,\ldots, \tag{12}$$

where, by definition, $R_{-1}\equiv X_{J\mathcal{H}}$ is a solution of the operator equation $J=[X_{J\mathcal{H}},\mathcal{H}]$, and

$$R_0\equiv R_0(J)=J,\quad R_1\equiv R_1(J)=[\mathcal{H},J],\ \ldots,\ R_n\equiv R_n(J)=[\mathcal{H},R_{n-1}(J)]. \tag{13}$$

The observables R_k, $k=0,1,2,\ldots$, were introduced in [9]. Next, we have defined

$$F_{2n+1}(J;J)\equiv Z^{-1}\sum_{ml}|J_{ml}|^2(e^{-\beta E_l}+e^{-\beta E_m})[\beta(E_m-E_l)]^{2n}$$
$$=\beta^{2n}\langle[R_nR_n^++R_n^+R_n]\rangle,\quad n=0,1,2,3,\ldots. \tag{14}$$

In particular,

$$F_0(J;J)=(J;J),\quad F_1(J;J)=\langle JJ^++J^+J\rangle,\quad F_2(J;J)=\beta\langle[[J^+,\mathcal{H}],J]\rangle,$$
$$F_3(J;J)=\beta^2\langle[J^+,\mathcal{H}][\mathcal{H},J]+[\mathcal{H},J][J^+,\mathcal{H}]\rangle. \tag{15}$$

The functionals (12) and (14) are used to generalize all the known inequalities used in the Approximating Hamiltonian method. Here we give the final results:

Generalized Harris inequality

$$F_{2n}(J;J)\le\frac{1}{2}F_{2n+1}(J;J)\le F_{2n}(J;J)+\frac{1}{12}F_{2n+2}(J;J). \tag{16}$$

The Brooks Harris inequality (8) is recovered when $n=0$.

Generalized Plechko inequalities

$$(2Z)^{-1}\sum_{ml}|J_{ml}|^2|e^{-\beta E_l}-e^{-\beta E_m}|[\beta(E_m-E_l)]^{2n}$$
$$\le\frac{1}{2}(J;J)^{1/p}\left\{Z^{-1}\sum_{ml}|J_{ml}|^2\frac{e^{-\beta E_l}-e^{-\beta E_m}}{\beta(E_m-E_l)}[\beta|E_m-E_l|]^{(2n+1)q}\right\}^{1/q}, \tag{17}$$

where $p,q>1$ and $1/p+1/q=1$.

One of the possible choices of p and q here is even integer $q=2k$ (hence, $p=2k/(2k-1)$) which leads to the set of **generalized Ginibre inequalities** ($k=1,2,3,\ldots$):

$$F_{2n}(J;J)\le\frac{1}{2}F_{2n+1}(J;J)\le F_{2n}(J;J)+\frac{1}{2}(J;J)^{(2k-1)/2k}[F_{2k(2n+1)}(J;J)]^{1/2k}. \tag{18}$$

At $n=0$ the above set reduces to a symmetric version of the inequalities obtained by Plechko [10]:

$$(J;J)\le\frac{1}{2}\langle JJ^++J^+J\rangle\le(J;J)+\frac{1}{2}(J;J)^{(2k-1)/2k}\beta(R_k;R_k)^{1/2k},\quad(k=1,2,3,\ldots). \tag{19}$$

Hence, in the particular case of $k = 1$ one obtains the Ginibre inequality (9).

Generalized Bogoliubov Jr. - Plechko - Repnikov inequalities are obtained from (17) when we choose odd $q = 2k + 1$, hence, $p = (2k + 1)/2k$, $k = 1, 2, 3, \ldots$:

$$\frac{1}{2}F_{2n+1}(J;J) \leq F_{2n}(J;J) + \frac{1}{2}(J;J)^{2k/(2k+1)}[F_{2(2nk+n+k)+1}(J;J)]^{1/(2k+1)}. \qquad (20)$$

At $n = 0$ these reduce to a symmetric version of the set of inequalities obtained by Bogoliubov Jr., Plechko and Repnikov [9]:

$$\frac{1}{2}\langle JJ^+ + J^+J\rangle \leq (J;J) + \frac{1}{2}(J;J)^{2k/(2k+1)}\{\beta^{2k}\langle R_kR_k^+ + R_k^+R_k\rangle\}^{1/(2k+1)}. \qquad (21)$$

The symmetric version of the inequality due to Bogoliubov Jr. (11) follows from here in the particular case of $k = 1$.

In [5], we show that under sufficiently mild conditions, each of the generalized upper bounds has the same form and order of magnitude with respect to the number of particles (or volume) for all the quantities derived by commutations of an intensive observable with the Hamiltonian of the system. The application of the generalized inequalities to a quantum spin model with separable attraction and the Dicke model of superradiance is given too.

2. Bounds on the fidelity susceptibility

Over the last decade there have been impressive theoretical advances concerning the concepts of entanglement and fidelity from quantum and information theory [11],[12], and their application in condensed matter physics, especially in the theory of critical phenomena and phase transitions, for a review see [13, 14]. These two concepts are closely related to each other.

The fidelity [15, 16] naturally appears in quantum mechanics as the absolute value of the overlap (Hilbert-space scalar product) of two quantum states corresponding to different values of the control parameters. The corresponding finite-temperature extension, defined as a functional of two density matrices, ρ_1 and ρ_2,

$$\mathcal{F}(\rho_1, \rho_2) = \mathrm{Tr}\sqrt{\rho_1^{1/2}\rho_2\rho_1^{1/2}}, \qquad (22)$$

was introduced by Uhlmann [17] and called fidelity by Jozsa [15].

Being a measure of the similarity between quantum states, both pure or mixed, fidelity should decrease abruptly at a critical point, thus locating and characterizing the phase transition. Different finite-size scaling behaviors of the fidelity indicate different types of phase transitions. The fidelity approach is basically a metric one and has an advantage over the traditional Landau-Ginzburg theory, because it avoids possible difficulties in identifying the notions of order parameter, symmetry breaking, correlation length, and so it is suitable for the study of different kinds of topological or Berezinskii-Kosterlitz-Thouless phase transitions.

The above mentioned decrease in the fidelity $\mathcal{F}(\rho_1, \rho_2)$, when the state ρ_2 approaches a quantum critical state ρ_1, is associated with a divergence of the fidelity susceptibility $\chi_F(\rho_1)$ which reflects the singularity of $\mathcal{F}(\rho_1, \rho_2)$ at that point. The fidelity susceptibility $\chi_F(\rho_1)$, which is the main object of this study, naturally arises as a leading-order term in the expansion of the fidelity for two infinitesimally close density matrices ρ_1 and $\rho_2 = \rho_1 + \delta\rho$. For simplicity, in our study [18] we consider the one-parameter family of Gibbs states

$$\rho(h) = [Z(h)]^{-1} \exp[-\beta H(h)], \tag{23}$$

defined on the family of Hamiltonians of the form $H(h) = T - hS$, where the Hermitian operators T and S do not commute in the general case, h is a real parameter, and $Z(h) = \mathrm{T}r \exp[-\beta H(h)]$ is the corresponding partition function. The fidelity susceptibility at the point $h = 0$ in the parameter space is defined as (see e.g. [19]):

$$\chi_F(\rho(0)) := \lim_{h\to 0} \frac{-2 \ln \mathcal{F}(\rho(0), \rho(h))}{h^2} = - \left. \frac{\partial^2 \mathcal{F}(\rho(0), \rho(h))}{\partial h^2} \right|_{h=0}. \tag{24}$$

To proceed with the calculations when the operators T and S do not commute, we introduce a convenient spectral representation. To simplify the problem, we assume that the Hermitian operator T has a complete orthonormal set of eigenstates $|n\rangle$, $T|n\rangle = T_n|n\rangle$, where $n = 1, 2, \ldots$, with non-degenerate spectrum $\{T_n\}$. In this basis the zero-field density matrix $\rho(0)$ is diagonal too, $\langle m|\rho|n\rangle = \rho_m \delta_{m,n}$, $m, n = 1, 2, \ldots$.

In [18], we derive the following expression for the spectral representation of the fidelity susceptibility in the general noncommutative case,

$$\chi_F(\rho) = \frac{\beta^2}{8} \sum_{m,n,m\neq n} \frac{\rho_n - \rho_m}{X_{mn}} \frac{|\langle n|S|m\rangle|^2}{X_{mn} \coth X_{mn}} + \frac{1}{4}\beta^2 \langle (\delta S^d)^2 \rangle_0. \tag{25}$$

which is convenient for the derivation of inequalities involving macroscopic quantities, like susceptibilities and thermal average values. Here $X_{mn} \equiv \beta(T_m - T_n)/2$, $\langle \cdots \rangle_0$ denotes the Gibbs average value at $h = 0$, $\delta S^d = S^d - \langle S^d \rangle_0$, where S^d is the diagonal part of the operator S, so that

$$\langle (\delta S^d)^2 \rangle_0 := \sum_m \rho_m \langle m|S|m\rangle^2 - \langle S \rangle_0^2. \tag{26}$$

Note that the first term in the right-hand side of (25) describes the purely quantum contribution to the fidelity susceptibility, since it vanishes when the operators T and S commute, while the second term represents the "classical" contribution.

Lower and upper bounds on the fidelity susceptibility follow by applying elementary inequalities for $(x \coth x)^{-1}$ to the summand in the above expression. Thus, we obtain an upper bound on $\chi_F(\rho)$ in the transparent form

$$\chi_F(\rho) \leq \frac{\beta^2}{4} (\delta S; \delta S)_0, \tag{27}$$

where $(\delta S; \delta S)_0$ is the Bogoliubov-Duhamel inner product of the self-adjoint operator δS with itself in the Gibbs ensemble with Hamiltonian $H(0) = T$. Note that the right-hand

side of the above inequality is proportional to the initial thermodynamic susceptibility:

$$(\delta S;\delta S)_0 = -\frac{N}{\beta}\frac{\partial^2 f[H(h)]}{\partial^2 h}\mid_{h=0} := \frac{N}{\beta}\chi_N, \tag{28}$$

where $f[H(h)]$ is the free energy density of the system described by the Hamiltonian $H(h)$ and χ_N is the susceptibility with respect to the field h.

On the other hand, by applying the elementary inequality $(x\coth x)^{-1} \geq 1-(1/3)x^2$ to the spectral representation for the fidelity susceptibility (25), we obtain the following lower bound

$$\chi_F(\rho) \geq \frac{\beta^2}{4}(\delta S;\delta S)_0 - \frac{\beta^3}{48}\langle[[S,T],S]\rangle_0. \tag{29}$$

The quality of the derived upper and lower bounds was tested in the simplest case of a single spin in the external magnetic field, subject to a transverse-field perturbation. Finally, these bounds were applied to two many-body quantum-mechanical models: the single impurity Kondo model and the Dicke model of superradiance. In conclusion, our lower (29) and upper (27) bounds indicate that for detection of a second order phase transition, with diverging in the thermodynamic limit susceptibility, the fidelity susceptibility per particle χ_F/N is as efficient as the usual susceptibility χ. This conclusion is in conformity with the commonly accepted view that quantum fluctuations are dominated by the thermal ones when $T_c > 0$. However, one should keep in mind that our results were derived under rather restrictive conditions on the spectrum of the Hamiltonian.

[1] R.B. Grifits "Rigorous results and theorems", in: *Phase Transition and Critical Phenomena, v.1, N.Y. Acad.Prsess, p.7 (1972).*

[2] Dyson F.J., Lieb E.H., Simon B., *J. Stat. Phys.,* ***18*** *(1978) 335.*

[3] A. Gelfert and W. Nolting, *J. Phys.: Cond. Matter* ***13*** *(2001) R505.*

[4] G. Röpstorff, *Comm. Math. Phys.,* ***53*** *(1977) 143.*

[5] J. G. Brankov and N. S. Tonchev, *Cond. Mat. Phys.* ***14*** *(2011) 13003:1-17.*

[6] Bogoliubov (Jr.) N.N., "A Method for Studying Model Hamiltonians" *(Pergamon Press, Oxford, 1972).*

[7] Harris A.B., *J. Math. Phys.,* ***8*** *(1967) No. 5, 1044.*

[8] Ginibre J., *Comm. Math. Phys.,* ***16*** *(1970) 310328.*

[9] Bogoliubov (Jr.) N.N., Plechko V.N., and Repnikov N.F., *Teor. Mat. Fiz.,* ***24*** *(1975) No. 3, 357 (in Russian).*

[10] Plechko V.N., *Teor. Mat. Fiz.,* ***28*** *(1976) No. 1, 127 (in Russian).*

[11] I. Bengtsson and K. Życzkowski, "Geometry of Quantum States: An Introduction to Quantum Entanglement" *Cambridge University Press, Cambridge, England, 2006.*

[12] L. Amico, R. Fazio, A. Osterloh and V. Vedral, *Rev. Mod. Phys.,* ***80*** *(2008) 517.*

[13] L. Amico and R. Fazio, *J. Phys. A: Math. Theor.,* ***42****, 504001 (2009).*

[14] S.-J. Gu, *Int. J. Mod. Phys. B.,* ***24*** *(2010) No 23, 4371.*

[15] R. Jozsa, *J. Mod. Optics,* ***41*** *(1994) 2315.*

[16] B. Schumacher, *Phys. Rev. A,* ***51*** *(1995) 2738.*

[17] A. Uhlmann, *Rep. Math. Phys.,* ***9*** *(1976) 273.*

[18] J. G. Brankov and N. S. Tonchev, *Phys. Rev. E* ***85*** *(2012) 031115 1-8.*

[19] V.R. Viera, *J. Phys.: Conf. Series,* ***213*** *(2010) 012005.*

PROSPECTS FOR INVESTIGATING DETERMINISTIC FRACTALS: EXTRACTING ADDITIONAL INFORMATION FROM SMALL-ANGLE SCATTERING DATA

A. Yu. Cherny[a], E. M. Anitas[a,b], V. A. Osipov[a], and A. I. Kuklin[a]
[a]Joint Institute for Nuclear Research, 141980 Dubna, Russia
[b]Horia Hulubei National Institute of Physics and Nuclear Engineering, RO-077125 Bucharest-Magurele, Romania

Fractals, one of the most beautiful and interesting groups of objects, have appeared in the scientific literature quite recently [1]. Right after that, the fractals attracted much attention of a broad community of investigators in various fields. Nearly at the same time, the connections were revealed between fractal structures and the intensities of small-angle neutron or X-ray scattering (see, e.g., reviews [2, 3] and references therein). In particular, it was shown that within the fractal region of a mass fractal, the SAS intensity decays in the momentum space, according to the power law

$$I(q) \propto q^{-D}, \tag{30}$$

where D is the fractal dimension. The majority of SAS studies focus on determining the fractal dimension and the edges of the fractal region, within which the object behaves as a fractal. For random (stochastic) fractals, it is rather difficult to extract more information from the SAS data, because the fine structure of spatial correlations of particles, forming the fractal, is usually smeared due to the randomness. Presently, various deterministic fractals can be artificially created due to a rapid progress in nanotechnologies. As has recently been shown [4, 5], deterministic fractals, being exact self-similar objects, allow us to obtain more information from the scattering data.

In [6, 7], we constructed the generalized 3D Cantor and Vicsek sets (Fig. 1), whose dimensions are controlled by the scaling factor of fractal. The SAS intensities from these deterministic fractals were calculated analytically, and the obtained results exhibit a number of general features common for deterministic mass fractals with a single scale [4, 5]. If the fractals, composing a sample, are randomly oriented and placed, then the SAS intensities represent minima and maxima superimposed on the power-law decay $I(q) \propto q^{-D}$ (the generalized power-law decay). In the reciprocal fractal region, the curve $I(q)q^D$ is approximately log-periodic with the period equal to the logarithm of the fractal scaling factor (Fig. 2), and this log-periodicity of the scattering curves is a consequence of the self-similarity of the fractal. As was shown in [4, 5, 6, 7], the minima and maxima amplitudes are damped with increasing fractal polydispersity, i.e., variance in fractal sizes in the sample. Physical reasons for such a behavior are quite clear: the fractal dimension dictates the power law $I(q) \propto q^{-D}$ for the intensity only on the average. Polydispersity smears the spatial correlations between the units composing the fractal and, hence, the intensity becomes smoother.

For a mass fractal with a single scale, one can extract a number of parameters from the scattering intensity even in the presence of polydispersity (Fig. 2):

(i) The fractal dimension from the generalized power-law decay.

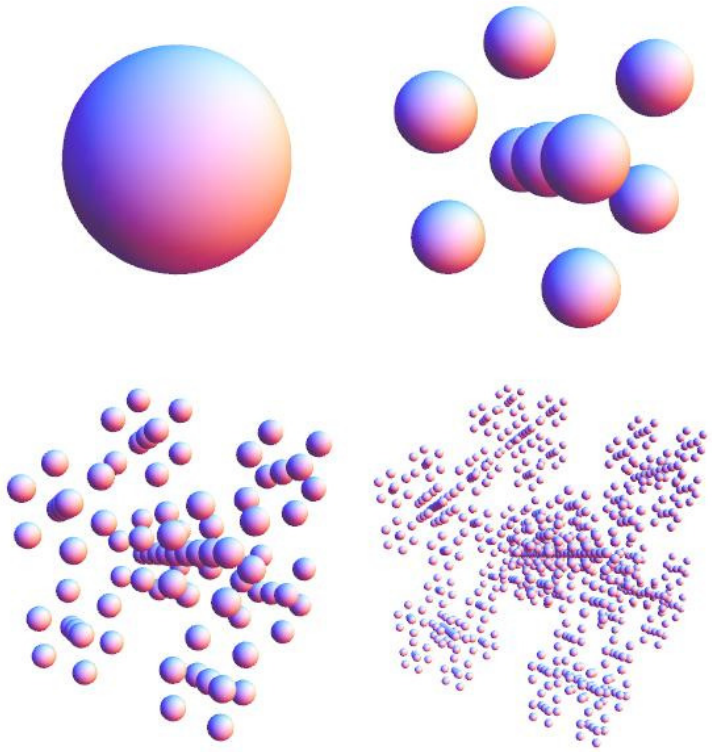

Figure 1: (Color online) The initiator and first three iterations for the generalized self-similar Vicsek fractal, a deterministic fractal immersed in 3D, at the scaling factor $\beta_{\rm s} = 1/6$.

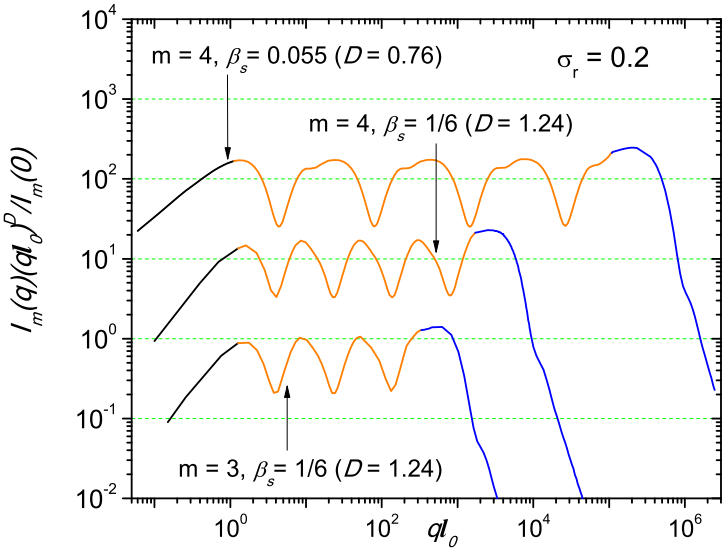

Figure 2: (Color online) The log-periodicity of the scaled SAS intensity $I(q)q^D$ in the fractal region of the generalized Vicsek sets. The period in the log-scale is equal to $\log_{10}(1/\beta_{\rm s})$. Here l_0 and $\sigma_{\rm r}$ are the average fractal size and its relative variance, respectively, and m is the iteration number.

(ii) The fractal scaling parameter from the period on the logarithmic scale.

(iii) The number of fractal iteration, which is equal to the number of periods of function $I(q)q^D$.

(iv) The lower and upper fractal edges from this diagram as the beginning and end of the "periodicity region". The edges allow us to estimate the fractal size and the smallest distance between fractal units in real space.

(v) The total number of structural units, of which the fractal is composed, by the relation $N_m = (1/\beta_s)^{mD}$, where m is the iteration number.

The analysis of SAS data for deterministic fractals represents an important step in the structural investigations of complex systems. One can expect that the required samples of deterministic fractals of higher quality will be obtained with the help of modern nanotechnologies and investigated by SAS in near future.

[1] B. B. Mandelbrot, *The Fractal Geometry of Nature* (Freeman, San-Francisco, 1982).

[2] J. Teixeira, *J. Appl. Cryst.* **21**, 781 (1988).

[3] P. W. Schmidt, *J. Appl. Cryst.* **24**, 414 (1991).

[4] A. Yu. Cherny, E. M. Anitas, V. A. Osipov and A. I. Kuklin, *Phys. Rev. E.* **84**, 036203 (2011).

[5] A. Yu. Cherny, E. M. Anitas, V. A. Osipov and A. I. Kuklin, *J. Phys. Conf. Ser.* **351**, 012020 (2012).

[6] A. Yu. Cherny, E. M. Anitas, A. I. Kuklin, M. Balasoiu and V. A. Osipov *J. Appl. Cryst.* **43**, 790 (2010).

[7] A. Yu. Cherny, E. M. Anitas, A. I. Kuklin, M. Balasoiu and V. A. Osipov *J. Surf. Invest.* **4**, 903 (2010).

OPTICAL AND DC CONDUCTIVITIES OF CUPRATES: SPIN-FLUCTUATION SCATTERING IN THE t-J MODEL

A. A. Vladimirov[a], D. Ihle[b], and N. M. Plakida[a,c]
[a]Joint Institute for Nuclear Research, 141980 Dubna, Russia
[b] Institut für Theoretische Physik, Universität Leipzig, D-04109, Leipzig, Germany
[c]Max-Planck-Institut für Physik komplexer Systeme, D-01187, Dresden, Germany

Studies of charge dynamics in superconducting cuprates provide valuable information concerning electron interaction with bosonic modes which is important for elucidating the mechanism of high-temperature superconductivity (HTSC). It is believed that electron interaction with the antiferromagnetic (AF) spin fluctuations has sufficient strength to mediate HTSC in cuprates and to explain various physical properties of cuprate materials (for a review see [1]). In the present concise report based on the published paper [2], we prove this point of view. We develop the microscopic theory of the optical conductivity $\sigma(\omega)$ within the t–J model and derive the generalized Drude law. The theory is based on the memory-function formalism which enables one to calculate directly the transport relaxation rate without using the Allen perturbation theory. The relaxation rate due to the decay of charge excitations into particle-hole pairs assisted by antiferromagnetic spin fluctuations is calculated in the mode-coupling approximation. The relaxation rate and the optical and dc conductivities are calculated in a broad region of doping and temperatures. The reasonable agreement of the theory with experimental data for cuprates proves an important role of spin-fluctuation scattering in the charge dynamics.

1. General theory

In the linear response theory of Kubo the optical conductivity is defined by the current–current relaxation function,

$$\sigma_{xx}(\omega) = \frac{i}{V}\left((J_x|J_x)\right)_\omega = \frac{1}{V}\int_0^\infty dt \mathrm{e}^{i\omega t}\int_0^\beta d\lambda \langle J_x(t-i\lambda)J_x\rangle, \tag{31}$$

where $V = Nv_0$ is the volume of the system. The current operator $J_x(t) = dP_x(t)/dt = -i[P_x, H]$ is defined by the time derivative of the polarization operator $P_x = e\sum_i R_i^x N_i$ where N_i is the number operator for electrons with the charge e and the x-component of the coordinate R_i^x at the site i (here $\beta = 1/T$, $\hbar = k_B = 1$). $\langle AB\rangle$ denotes the equilibrium statistical average for a system with the Hamiltonian H. Using the Mori projection technique the optical conductivity (31) can be written in the form of the generalized Drude law:

$$\sigma_{xx}(\omega) \equiv \sigma(\omega) = \frac{\omega_{\mathrm{pl}}^2}{4\pi}\quad\frac{m}{\widetilde{m}(\omega)}\quad\frac{1}{\widetilde{\Gamma}(\omega) - i\omega}. \tag{32}$$

Here the effective optical mass $\widetilde{m}(\omega)/m = 1 + \lambda(\omega)$ and the relaxation rate $\widetilde{\Gamma}(\omega) = \Gamma(\omega)/[1+\lambda(\omega)]$ are given by the real $M'(\omega)$ and the imaginary $M''(\omega)$ parts of the memory

function: $\lambda(\omega) = M'(\omega)/\omega, \quad \Gamma(\omega) = M''(\omega)$. The memory function

$$M(\omega) = ((F_x|F_x))^{(\text{proper})}_{\omega}(1/\chi_0), \tag{33}$$

is determined by the relaxation function of the force operators $F_x = [J_x, H]$. The static susceptibility χ_0 is related to the plasma frequency $\omega^2_{\text{pl}} = 4\pi\chi_0/V \equiv N_{\text{eff}}\,\omega^2_{0,\text{pl}}$ and the effective number of charge carriers N_{eff} is determined by the sum rule:

$$\frac{1}{\pi}\int_0^\infty d\omega \text{Re}\,\sigma_{xx}(\omega) = \frac{\chi_0}{2V} = \frac{i}{2V}\langle[J_x, P_x]\rangle = \frac{N_{\text{eff}}\text{e}^2}{2mv_0}. \tag{34}$$

2. Optical conductivity for the t-J model

We consider the t–J model written in terms of the Hubbard operators (HOs):

$$H = -\sum_{i\neq j,\sigma} t_{ij} X_i^{\sigma 0} X_j^{0\sigma} - \mu\sum_{i\sigma} X_i^{\sigma\sigma} + \frac{1}{4}\sum_{i\neq j,\sigma} J_{ij}\left(X_i^{\sigma\bar{\sigma}} X_j^{\bar{\sigma}\sigma} - X_i^{\sigma\sigma} X_j^{\bar{\sigma}\bar{\sigma}}\right), \tag{35}$$

where t_{ij} is the hopping integral and J_{ij} is the exchange interaction. The HOs $X_i^{\alpha\beta} = |i,\alpha\rangle\langle i,\beta|$ describe transitions between three possible states at a site i on a square lattice: an empty state $|i,\alpha\rangle = |i,0\rangle$ and a singly occupied state $|i,\alpha\rangle = |i,\sigma\rangle$ with spin $\sigma/2 = \pm 1/2$, $(\bar{\sigma} = -\sigma)$. The number and spin operators are given by: $N_i = \sum_\sigma X_i^{\sigma\sigma}$, $S_i^\sigma = X_i^{\sigma\bar{\sigma}}$, $S_i^z = (1/2)\sum_\sigma \sigma\, X_i^{\sigma\sigma}$. The chemical potential μ is determined from the equation for the average electron density $n = \langle N_i\rangle = 1 - \delta$, where $\delta = \langle X_i^{00}\rangle$ is the hole concentration.

The relaxation rate $\Gamma(\omega) = M''(\omega)$ is calculated in the mode-coupling approximation assuming an independent propagation of electron and charge-spin excitations:

$$\begin{aligned}\Gamma(\omega) &= \frac{(e^{\beta\omega}-1)}{\chi_0\,\omega}\frac{2\pi\,\text{e}^2}{N}\sum_{\mathbf{k},\mathbf{q}} g_x^2(\mathbf{k},\mathbf{k}-\mathbf{q})\iiint_{-\infty}^{\infty} d\omega_1 d\omega_2 d\omega_3 n(\omega_1)[1-n(\omega_2)]N(\omega_3) \\ &\times \chi''_{cs}(\mathbf{q},\omega_3)A(\mathbf{k},\omega_1)A(\mathbf{k}-\mathbf{q},\omega_2)\,\delta(\omega_2-\omega_1-\omega_3+\omega),\end{aligned} \tag{36}$$

where $n(\omega) = (\exp\beta\omega + 1)^{-1}$ and $N(\omega) = (\exp\beta\omega - 1)^{-1}$. The momentum dependent (transport) vertex is given by $g_x(\mathbf{k},\mathbf{k}-\mathbf{q}) = v_x(\mathbf{k})\,t(\mathbf{k}-\mathbf{q}) - v_x(\mathbf{k}-\mathbf{q})\,t(\mathbf{k}) - (1/2)J(\mathbf{q})\,[v_x(\mathbf{k}) - v_x(\mathbf{k}-\mathbf{q})]$, where $t(\mathbf{k})$ and $J(\mathbf{q})$ are the Fourier transforms of the hopping integral and the exchange interaction, and $v_x(\mathbf{k}) = -\partial t(\mathbf{k})/\partial k_x$ is the electron velocity. The spectral function for the charge-spin excitations is determined by the corresponding Green functions (GFs): $\chi''_{cs}(\mathbf{q},\omega) = -(1/\pi)\text{Im}\,[(1/4)\langle\langle N_\mathbf{q}|N_{-\mathbf{q}}\rangle\rangle_\omega + \langle\langle \mathbf{S}_\mathbf{q}|\mathbf{S}_{-\mathbf{q}}\rangle\rangle_\omega$. The spectral function of electronic excitations is defined by the imaginary part of the single-particle GF: $A(\mathbf{k},\omega) = -(1/\pi)\,\text{Im}\langle\langle X^{0\sigma}_\mathbf{k} \mid X^{\sigma 0}_\mathbf{k}\rangle\rangle_\omega$.

3. Results and discussion

In computations the model for the spin susceptibility $\langle\langle \mathbf{S}_\mathbf{q}|\mathbf{S}_{-\mathbf{q}}\rangle\rangle_\omega$ found in Ref. [3] was used. The single-electron spectral function was approximated by the expression: $A(\mathbf{k},\omega) = Q\,\delta(\omega - \tilde{\varepsilon}_\mathbf{k})$, where $Q = 1 - n/2$ and the quasiparticle excitation spectrum is given by $\tilde{\varepsilon}_\mathbf{k} = -4Q[t\,\alpha_1\gamma(\mathbf{k}) + t'\alpha_2\,\gamma'(\mathbf{k}) + t''\alpha_2\,\gamma''(\mathbf{k})] - \mu$. Here t and t', t''

are the hopping parameters for the nearest and further-distant neighbors, respectively, renormalized by the short-range AF correlation parameters α_i (see [4]) and $\gamma(\mathbf{k}) = (1/2)(\cos ak_x + \cos ak_y)$, $\gamma'(\mathbf{k}) = \cos ak_x \cos ak_y$ and $\gamma''(\mathbf{k}) = (1/2)(\cos 2ak_x + \cos 2ak_y)$. Using these approximations the relaxation rate (36), the optical conductivity (32) and the electrical resistivity $\rho = 1/\sigma(0)$ were calculated and compared with experiments.

The relaxation rate $\Gamma(\omega)$ is compared in Fig. 3 (a) with the optical data for $YBa_2Cu_3O_{6.5}$ ($YBCO_{6.5}$) [5]. In the frequency region $\omega \leq 1500$ cm^{-1} our results are close to the experimental values. At zero frequency, the relaxation rate is related to the elec-

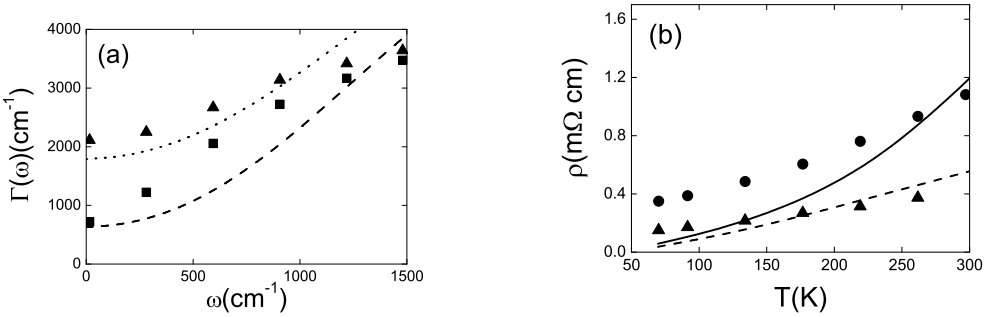

Figure 3: (a) Relaxation rate $\Gamma(\omega)$ at $\delta = 0.09$ for $T \approx 140$ K (dashed) and $T \approx 230$ K (dotted) in comparison with experimental data for $YBCO_{6.5}$ shown by symbols: squares for $T = 147$ K and triangles for $T = 244$ K. (b) Temperature dependence of the resistivity $\rho(T)$ for $LSCO_\delta$ at $\delta = 0.08$ (solid) and $\delta = 0.17$ (dashed) in comparison with the experimental data shown by symbols.

trical resistivity by $\Gamma(0)/t = N_{\rm eff} A\rho(T)$ where $A = \omega_{0\rm pl}^2/(4\pi t) = e^2/(mv_0 t)$. In Fig. 3 (b), we compare the resistivity with experimental data for $La_{2-\delta}Sr_\delta CuO_4$ ($LSCO_\delta$) [6] for the underdoped ($\delta = 0.08$) and nearly optimally doped ($\delta = 0.17$) samples. A reasonable agreement is observed at high temperatures, while at low temperatures our values are smaller. An additional scattering mechanism, such as impurity scattering and electron-phonon interaction, should be invoked to explain the experimental data.

To conclude, within the proposed theory, we are able to obtain a reasonable agreement with experiments on cuprates for the relaxation rate, the optical conductivity, and the resistivity in broad regions of temperatures and doping. This proves the essential role of AF spin fluctuations in the charge dynamics of cuprates. From our results we conclude that spin-fluctuations induced by the kinematic interaction for the HOs should give a substantial contribution to the d-wave pairing in cuprates, as it has been shown recently in Ref. [7].

[1] N. M. Plakida, *High-Temperature Cuprate Superconductors* (Springer Series in Solid-State Sciences, Vol. 166, Springer-Verlag, Berlin, 2010) – 570 pp.

[2] A. A. Vladimirov, D. Ihle, and N. M. Plakida, Phys. Rev. B **85**, 224536 (2012).

[3] A. A. Vladimirov, D. Ihle, and N. M. Plakida, Phys. Rev. B **80**, 104425 (2009).

[4] N. M. Plakida and V. S. Oudovenko, Phys. Rev. B **59**, 11949 (1999).

[5] J. Hwang, J. Yang, T. Timusk, et al., Phys. Rev. B **73**, 014508 (2006).

[6] G. S. Boebinger, Y. Ando, A. Passner, et al., Phys. Rev. Lett. **77**, 5417 (1996).

[7] N. M. Plakida and V. S. Oudovenko, arXiv:1391.4347 [cond-mat.str-el].

ON UNIVERSAL EXIT PROBABILITIES IN THE TASEP

S.S. Poghoyan, A.M. Povolotsky, V.B. Priezzhev

The totally asymmetric simple exclusion process (TASEP) was a subject of numerous investigations [1, 2, 3, 4]. Full information on its space-time evolution can be presented in terms of the correlation functions for positions of particles at different time moments. The first result on the one-point current distribution was obtained in [5] and generalized in [6, 7]. Multi-point correlation functions of particle positions at a fixed time moment were addressed in [8, 9, 10, 11]. The correlation functions describing particles at different space-time positions were obtained in [12, 13, 14, 15].

In the scaling limit the correlation functions become universal scaling functions of the Kardar-Parisi-Zhang (KPZ) universality class [16]. The distributions of fluctuations of space-time particle positions converge to those of the universal random processes, like Airy_1,[8], Airy_2, [17], e.t.c, which depend only on the global form of the initial particle density profile.

All the mentioned results were obtained within restricted space-time domains which required ordering of the space and time coordinates of the events described by the correlation functions. Below we present the most general space-time correlation functions, where all the restrictions on the time coordinates are removed. The restrictions on spacial coordinates still remain. They ensure that all the points under consideration belong to a space-like path [18]. Violation of this restriction changes drastically the nature of correlations, which seems to be a physically motivated obstacle for further progress. The result for the scaling limit of the functions obtained show that the Airy_2 universality holds within the whole extended space-like domain. The details of calculations can be found in [50].

Consider the system of particles on the 1D integer lattice. At any time moment a configuration of particles is specified by a set of N strictly increasing integers, $(x_1 > x_2 > \dots)$, denoting particle coordinates. They evolve in a discrete time $t \in \mathbb{Z}$, according to the TASEP [1] dynamical rules: (i) A particle takes a step forward, $(x_i \to x_i + 1)$, with probability p and stays at the same site, $(x_i \to x_i)$, with probability $q \equiv 1 - p$ provided that the target site is empty, $(x_i{+}1 \neq x_{i-1})$. (ii) If the next site is occupied, $(x_i{+}1 = x_{i-1})$, the particle stays with probability 1. (iii) The backward sequential update is used: at each time step the positions x_i of all particles are updated one by one, in the order of increasing of particle index: $i = 1, 2, 3, \dots$. These dynamical rules define transition probabilities for a Markov chain constructed on the set of particle configurations. Given initial conditions, one can inquire for probabilities of various events in the course of the Markov evolution. In present paper, we are interested in the correlation functions which are the exit probabilities associated with a few specified particles and given space-time positions.

To define exit probability for a single particle performing 1D asymmetric random walk, consider a decomposition of the space-time 2D lattice into two complementary subsets $\Omega \bigcup \bar{\Omega} = \mathbb{Z}^2$. Given a random walk having started at the point $(x^0, t^0) \in \Omega$, the exit probability referring to Ω is a probability distribution of subsets of the boundary of Ω from which the particle exits Ω. The exit probabilities are meaningful for boundaries

which having been left behind by a particle can never be visited again. These boundaries can be constructed as follows:

Definition 1 *The boundary $\mathcal{B}$ is an infinite countable subset of $\mathbb{Z}^2$, $\mathcal{B} = \{b(\tau) \in \mathbb{Z}^2\}_{\tau\in\mathbb{Z}}$, with the following staircase-like structure. Let $b(\tau) = (x, t)$. Then the next point of the boundary will be either $b(\tau + 1) = (x - 1, t)$ or $b(\tau + 1) = (x, t + 1)$, for any $\tau \in \mathbb{Z}$. A natural integer variable τ increasing along the boundary from north-east to southwest can be chosen as $\tau = t - x, (x, t) \in \mathcal{B}$.*

More generally, one can consider a collection of embedded sets $\Omega_1 \subset \Omega_2 \subset \ldots$, with boundaries $\mathcal{B}_1, \mathcal{B}_2, \ldots$ and look for the joint distribution of successive exits from these boundaries.

The idea of exit probabilities for N particles undergoing the TASEP evolution on 1D lattice generalizes the single-particle picture. The concept of boundary can be generalized to N-boundary:

Definition 2 *Given boundary $\mathcal{B}$, the N-boundary $\mathcal{B}_N \subset \{1, \ldots, N\} \times \mathbb{Z}$, is defined as a disjoint union of N copies of $\mathcal{B}$, $\boldsymbol{\mathcal{B}}_N = \bigsqcup_{k=1}^{N} \mathcal{B}_k$, where the copy $\mathcal{B}_k = \{b_k(i)\}_{i\in\mathbb{Z}^2}$ associated with k-th particle is shifted by $(k - 1)$ steps back with respect to the first one in the horizontal (spacial) direction of space-time plane, $b_k(i) = (x(i) - k + 1, t(i))$, where $k = 1, \ldots, N$.*

The N-boundary is a generalization of the line with fixed time coordinate and of the set of lines with fixed space coordinates, which where the probability spaces used in [13, 14] and in [15], respectively. To specify from which to which point sets the system can pass in the course of the TASEP evolution, we also need a relation between subsets of $\{1, \ldots, N\}\times\mathbb{Z}^2$.

Definition 3 *Let $\Omega, \Omega' \subset \{1, \ldots, N\} \times \mathbb{Z}^2$. We say that the relation $\Omega \prec \Omega'$ holds, if for any $(x_k, t_k) \in \Omega$ and any $(x'_k, t'_k) \in \Omega'$ we have $(x'_k, t'_k) \in \{(x, t) : t \geq t_k\} \bigcup \{(x, t) : x > x_k\}$.*

The subindices denote the variable from the set $\{1, \ldots, N\}$ and are associated with the number of a particle.

As it was explained in [15], a space-time trajectory of a particle starting from the point preceding a given boundary, eventually transverses the boundary with the probability one. The question we address is: What is the probability for the trajectory to go from a given subset of the boundary? More generally we address the same question in connection with a collection of particles and a set of points at several boundaries.

To be specific, consider the TASEP evolution of N particles governed by the dynamical rules (i)-(iii). Let the initial configuration $\mathbf{x^0}$ be defined by

$$x_i^0 = -i + 1, \;\; i = 1, \ldots, N. \tag{37}$$

Let us fix a collection of N-boundaries, $\boldsymbol{\mathcal{B}}^1, \ldots, \boldsymbol{\mathcal{B}}^m$, $m > 0$, such that $\mathbf{x^0} \prec \boldsymbol{\mathcal{B}}^\mathbf{1} \prec \cdots \prec \boldsymbol{\mathcal{B}}^\mathbf{m}$, and fix the one-particle boundaries $\mathcal{B}_{N_1}^{k_1}, \ldots, \mathcal{B}_{N_l}^{k_l}$ within the N-boundaries. Here the upper indices $1 = k_1 \leq \cdots \leq k_l = m$ refer to the number of N-boundary, the lower indices, $N_l \leq \cdots \leq N_1 \equiv N$, to the particle number, and $l \geq m$. We suggest that at least one particle is fixed at each N-boundary, i.e. either $k_{i+1} = k_i$ or $k_{i+1} = k_i + 1$.

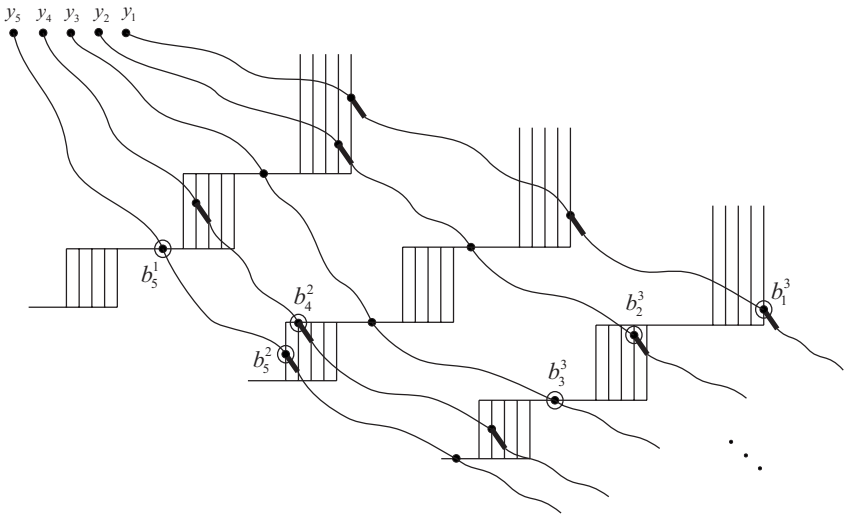

Figure 1: Trajectories of five TASEP particles traversing three 5-boundaries. Black segments emphasize that particles make a compulsory step forward at the sites belonging to vertical parts of boundaries from which the exits occur. The exits included into the correlation function with $N_1 = N_2 = 5, N_3 = 4, N_4 = 3, N_5 = 2, N_6 = 1$ and $k_1 = 1, k_2 = k_3 = 2, k_4 = k_5 = k_6 = 3$ are shown in circles.

We also require that equality $N_i = N_{i+1}$ for some i suggests that $k_{i+1} = k_i + 1$, i.e. two subsequent space-time points chosen for one particle should be put onto subsequent N-boundaries, and no other particles with a number less than N_i can be fixed at the N-boundary k_i. Let space-time positions of points $b_n^k(i)$ within the corresponding boundary $\mathcal{B}_n^k$ be indexed by index $i \in \mathbb{Z}$ in the same way as in Defs.1,2. The quantity of interest is the joint probability distribution $P(i_1 < a_1, \ldots, i_l < a_l)$ of the points $(b_{N_1}^{k_1}(i_1), \ldots, b_{N_l}^{k_l}(i_l))$ from which the space-time trajectories of particles $N_1, \ldots, N_l$ make steps when leaving the boundaries $(\mathcal{B}_{N_1}^{k_1}, \ldots, \mathcal{B}_{N_l}^{k_l})$, respectively (see Fig.1).

The first main result can be stated as the following theorem.

Theorem 1

Under the above conditions the joint probability distribution of exit points is given by the Fredholm determinant

$$P(i_1 < a_1, \ldots, i_l < a_l) = \det(\mathbb{I} - \eta_a K \eta_a)_{l^2(\{\mathcal{B}_{N_1}^{k_1}, \ldots, \mathcal{B}_{N_l}^{k_l}\})} \tag{38}$$

with the kernel

$$\begin{aligned} K(b_{N_i}^{k_i}, b_{N_j}^{k_j}) &= \oint_{\Gamma_1} \frac{dv}{2\pi \mathrm{i} v} \oint_{\Gamma_{0,v}} \frac{dw}{2\pi \mathrm{i} w} \frac{\frac{(1-p(\frac{w-1}{w}))^{t_i}}{(1-p(\frac{v-1}{v}))^{t_j}} \frac{(w-1)^{N_i}}{(v-1)^{N_j}} \frac{w^{x_{N_i}}}{v^{x_{N_j}}}}{(w-v)(1/v + 1/\pi_2 - 1)} \\ &- \mathbb{I}(N_2 > N_1) \oint_{\Gamma_{0,1}} \frac{dw}{2\pi \mathrm{i} w^2} \frac{(1-p(\frac{w-1}{w}))^{t_i - t_j} w^{x_{N_i} - x_{N_j}}}{(w-1)^{N_j - N_i}(1/v + 1/\pi_2 - 1)}. \end{aligned}$$

where $\eta_a = \mathbb{I}(i_1 \geq a_1) \times \cdots \times \mathbb{I}(i_1 \geq a_m)$, $b_{N_i}^{k_i} = (x_{N_i}, t_{N_i}) \in \mathcal{B}_{N_i}^{k_i}$, $i, j = 1, \ldots, l$ *and* $\pi_2 = 1, p$ *is the probability of step from the boundary* $\mathcal{B}_{N_j}^{k_j}$ *at the point* $b_{N_j}^{k_j}$.

It follows from the above construction of boundaries that the only constraint on the space-time points $b^{k_i}_{N_i}(\tau_i)$ is that on the spacial coordinated $(x^{k_1}_{N_1}(i_1) \le \cdots \le x^{k_l}_{N_l}(i_l))$, where the equality may hold only when $N_i = N_{i+1}$. This is the space like condition mentioned above.

To look at the distribution in a scaling limit, let us introduce variable change $(x,t) \to (\chi,\theta)$:

$$\chi = (t-x)/L, \qquad \zeta = (t+x)/L \tag{39}$$

and consider a limit $L \to \infty$, as χ and ζ are fixed. According to Def.1, the variable $\tau = \chi L$ can be used to enumerate points of any boundary. Let us introduce a differentiable function $\zeta(\chi,\theta)$ which defines a one-parameter family of curves $\zeta = \zeta(\chi,\theta)$ spanning the whole space-time plane as θ varies in $\mathbb{R}$. As the parameter χ runs in $\mathbb{R}$, it defines a point at a particular curve corresponding to some fixed value of θ. The continuous curves are used to approximate the boundaries at the discrete lattice, see Fig.2. Hence, the properties of $\zeta(\chi,\theta)$ follow from the properties of boundaries. Specifically, we suggest that

$$|\partial\zeta(\chi,\theta)/\partial\chi| \le 1 \qquad \text{and} \qquad (\partial/\partial\theta - \partial/\partial\chi)\,\zeta(\chi,\theta) \ge 1. \tag{40}$$

We now suppose that for $k = 1,\dots,m$ the boundaries $\mathcal{B}^k_1$ approximate the curves corresponding to a fixed set $(\theta_1,\dots,\theta_m)$:

$$b^k_1([L\chi]) = L\cdot((\zeta(\chi,\theta_k)-\chi)/2, (\zeta(\chi,\theta_k)+\chi)/2) + o(L^\sigma), \tag{41}$$

where the notation [ ] is for the integer part of a real number and the correction term should not contribute on a characteristic fluctuation scale, i.e. $\sigma = 1/3$. For technical purposes we also suggest that the correction term is uniform over the boundary. These boundaries correspond to the first particle. For a general particle with the number $n = [L\nu]$ we have to consider the boundary $\mathcal{B}^k_n$ shifting the spacial coordinate by $n-1$ steps backward:

$$b^k_n([L\chi]) = L\cdot((\zeta(\chi,\theta_k)-\chi)/2 - \nu, (\zeta(\chi,\theta_k)+\chi)/2) + o(L^\sigma). \tag{42}$$

Note that in the large scale, $x \sim n \sim t \sim L \to \infty$, the trajectories of particles are deterministic defined by the relation

$$\sqrt{p(\zeta(\chi,\theta)+\chi)} - \sqrt{(\zeta(\chi,\theta)-\chi)} - \sqrt{2q\nu} = 0, \tag{43}$$

which uniquely fixes value of χ given those of θ and ν, provided that the corresponding curve passes through the rarefaction fan defined by

$$\chi \le \zeta(\chi,\theta) \le \chi(1+p)/(1-p). \tag{44}$$

Let us consider a path in the $\theta-\nu$ plane:

$$\theta = \theta(r), \qquad \nu = \nu(r), \qquad r \in \mathbb{R}, \tag{45}$$

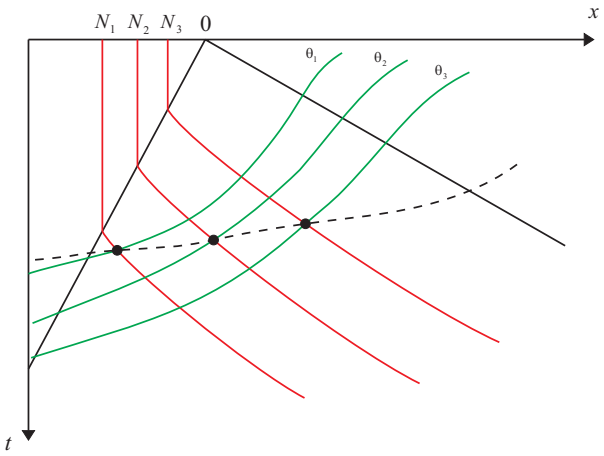

Figure 2: Exit probabilities on a space-like path in x-t plane. The wedge bounded by black straight lines is the rarefaction fan area. The deterministic trajectories of particles with numbers N_1, N_2, N_3 are shown in red. The green lines are boundaries with coordinates $x = L((\zeta(\theta_i, \chi) - \chi)/2 - \nu_i)$ and $t = L(\zeta(\theta_i, \chi) + \chi)/2$, where $i = 1, 2, 3$, corresponding to three fixed values of θ: $\theta_1 < \theta_2 < \theta_3$. Dashed line is the projection of the path $(\nu(r), \theta(r))$ to x-t plane: $x = L((\zeta(r) - \chi(r))/2 - \nu(r))$, $t = L(\zeta(r) + \chi(r))/2$. The black dots are the points where exits occur.

with differentiable functions $\theta(r)$ and $\nu(r)$, such that

$$\partial\theta/\partial r \geq 0, \qquad \partial\nu/\partial r \leq 0, \qquad \text{and} \qquad \partial\theta/\partial r - \partial\nu/\partial r \geq 1. \tag{46}$$

We select m points at the path, $r = r_1, \ldots, r_m$, so that the integers $N_1, \ldots, N_m$ from Theorem 1 are given by $N_i = [L\nu(r_i)]$, and $\theta_i = \theta(r_i)$. The inequalities (46) then guarantee that the constraints on $k_1, \ldots, k_m$ and $N_1, \ldots, N_m$ from Theorem 1 are satisfied and together with non-crossing of particle trajectories ensure that the points of this path accessible for the particle trajectories with nonzero probability form space-like configurations.

Substituting the functions $\theta(r)$ and $\nu(r)$ into (43) we obtain an equation which, given r, can be resolved with respect to χ. Now we turn to the fluctuations of these points referred to the boundaries and particle numbers separated by the distances of an order of correlation length from each other. Suppose that

$$r_i = r_0 + u_i L^{-1/3}. \tag{47}$$

The corresponding values of χ are given by their deterministic parts $\chi(r_i)$ plus a random variable of an order of fluctuation scale

$$\chi_i = \chi(r_i) + \xi_L(u_i) L^{-2/3}. \tag{48}$$

In the second theorem, we show that the random variable $\xi_L(u)$ converges to the universal Airy_2 process for a class boundaries, which can be approximated by (41)-(42).

Theorem 2

The following limit holds in a sense of finite-dimensional distributions:

$$\lim_{L\to\infty} \xi_L = \kappa_f \mathcal{A}_2(\kappa_c u), \tag{49}$$

where $\mathcal{A}_2$ is the Airy_2 *process characterized by multipoint distributions:*

$$\begin{aligned}\mathrm{Prob}(\mathcal{A}_2(u_1) < s_1, \ldots, \mathcal{A}_2(u_m) < s_m) \\ = \det\left(\mathbb{I} - \eta_s K_{\mathrm{Airy}_2}\eta_s)\right)_{L^2(\{n_1,\ldots,n_m\}\times\mathbb{R})}.\end{aligned} \tag{50}$$

where in the r.h.s. we have the extended Airy kernel,

$$\begin{aligned}K_{\mathrm{Airy}_2} \quad & (\xi_1,\zeta_1;\xi_2,\zeta_2) \\ & = \begin{cases} \int_0^\infty d\lambda e^{\lambda(\xi_2-\xi_1)}\mathrm{Ai}(\lambda+\zeta_1)\mathrm{Ai}(\lambda+\zeta_2), & \xi_2 \le \xi_1 \\ -\int_{-\infty}^0 d\lambda e^{\lambda(\xi_2-\xi_1)}\mathrm{Ai}(\lambda+\zeta_1)\mathrm{Ai}(\lambda+\zeta_2), & \xi_2 > \xi_1 \end{cases},\end{aligned} \tag{51}$$

The model dependent constants κ_c and κ_f defining the correlation and fluctuation scales, respectively, are given by

$$\begin{aligned}\kappa_c &= \frac{p^{1/6}\left(\sqrt{\omega}-\sqrt{p\gamma}\right)^{-1/3}\left(\sqrt{p\omega}-\sqrt{\gamma}\right)^{-1/3}}{2\gamma^{1/6}\omega^{1/6}\left(\sqrt{p\gamma}(1+\zeta^{(0,1)}(r_0))+\sqrt{\omega}(1-\zeta^{(0,1)}(r_0))\right)} \\ &\times \Big[q\nu'(r_0)\left(\zeta(r_0)-\chi(r_0)\zeta^{(0,1)}(r_0)\right)\left(\sqrt{p\omega}-\sqrt{\gamma}\right)^{-1} \\ &\qquad -\theta'(r_0)\zeta^{(1,0)}(r_0)\left(\sqrt{p\omega}-\sqrt{\gamma}\right)\Big]\end{aligned} \tag{52}$$

$$\kappa_f = \frac{\left(\sqrt{p\omega}-\sqrt{\gamma}\right)^{1/3}\left(\sqrt{p\gamma}(1+\zeta^{(0,1)}(r_0))+\sqrt{\omega}(1-\zeta^{(0,1)}(r_0))\right)}{2p^{1/6}\omega^{1/3}\gamma^{1/3}\left(\sqrt{\omega}-\sqrt{p\gamma}\right)^{2/3}}, \tag{53}$$

where we denote $\zeta(r) \equiv \zeta(\theta(r),\chi(r))$, $\zeta^{(1,0)}(r_0)$ ($\zeta^{(0,1)}(r_0)$) is the derivative of the function $\zeta(\theta,\chi)$ with respect to the first (second) argument at the point $(\theta(r_0),\chi(r_0))$, and the parameters γ and ω are defined by $\gamma = (\zeta(r_0)-\chi(r_0))/2$ and $\omega = (\zeta(r_0)+\chi(r_0))/2$.

The non-universal constants κ_f and κ_c are the most general ones for the TASEP with backward update. They depend not only on the macroscopic space-time location defined by $\zeta(r_0)$ and $\chi(r_0)$, but also on the local slope and local density of the boundaries at this point via the derivatives $\zeta^{(0,1)}(r_0)$ and $\zeta^{(1,0)}(r_0)$) respectively. Particular cases studied before can easily be restored from the expressions obtained. For example, for a purely spacial boundary used for measuring particle coordinates at fixed time we can take $\zeta(\theta,\chi) = 2t-\chi$, while the case of current correlation functions [15] corresponds to $\zeta(\theta,\chi) = 2x+\chi$. For the space-like correlation functions of particle coordinates studied in [13, 14] we take $\zeta(\theta,\chi) = 2\theta-\chi$, and the tagged particle case [12] corresponds to $\nu'(r) = 0$.

[1] Liggett T M, 1999 *Stochastic interacting systems: contact, voter and exclusion processes* (Berlin: Springer)

[2] Spohn H, 1991 *Large Scale Dynamics of Interacting Particles* (Berlin: Springer)

[3] B. Derrida, Phys. Rep. **301** 65 (1998).

[4] G.M. Schütz, in Phase Transitions and Critical Phenomena Vol. 19, edited by C. Domb and J.L. Lebowitz (Academic Press, London, 2001).

[5] Johansson K, 2000 *Comm. Math. Phys.* **209** 437

[6] Rákos A and Schütz G M, 2005 *J. Stat. Phys.* **118** 511

[7] Nagao T and Sasamoto T, 2004 *Nucl. Phys. B* **699** 487

[8] Sasamoto T, 2005 *J. Phys. A* **38** L549

[9] Borodin A, Ferrari P L, Prähofer M and Sasamoto T, 2007 *J. Stat. Phys.* **129** 1055

[10] Borodin A, Ferrari P L and Prähofer M, 2007 *Int. Math. Res. Papers* **2007** rpm002

[11] Borodin A, Ferrari P L and Sasamoto T, 2008 *Comm. Pure Appl. Math.* **61** 1603-1629

[12] Imamura T and Sasamoto T, 2007 *J. Stat. Phys.* **128** 799

[13] Borodin A and Ferrari P L, 2008 *Electron. J. Probab.* **13** 1380-1418

[14] Borodin A, Ferrari P L and Sasamoto T, 2008 *Comm. Math. Phys.* **283** 417

[15] Povolotsky A M, Priezzhev V B and Schütz G M, *J. Stat. Phys.* **142** 754

[16] Kardar M, Parisi G, Zhang Y-C, 1986 *Phys. Rev. Lett.* **56** 889892

[17] Praehofer M and Spohn H, 2004 *J. Stat. Phys.* **115** 255

[18] Ferrari P L, 2008 *J. Stat. Mech.* P07022

[19] S. S.Poghosyan, A. M. Povolotsky and V. B. Priezzhev, 2012 *J. Stat. Mech.* P08013.

Exact critical exponent for two-dimensional k-leg watermelon

V. S. Poghosyan and V. B. Priezzhev

Introduction. Enumeration of spanning trees on d–dimensional grids is a classical problem of the combinatorial graph theory. According to the Kirchhoff theorem[1], the number of spanning tree subgraphs on a lattice is given by minors of the discrete Laplacian matrix, Δ, of this lattice. Considering a modified matrix, Δ', which differs from Δ by a finite number of elements one can define local correlation functions of spanning trees in any dimension. Besides the combinatorial methods, in the two–dimensional case the conformal invariance allows one to evaluate the nonlocal correlations of special geometry in the spanning tree ensembles. For instance, using a mapping of the q–state Potts model to the Coulomb gas, and taking the limit $q \to 0$ Saleur and Duplantier [2] found the correlation function $W_k(r)$ of a k–path "connectivity" in the spanning tree. The k–path connectivity is defined as follows. Given two lattice points A and B separated by the distance r, one can find k paths along branches of the spanning tree from the vicinity of the point A to that of the point B. Such a topology is called in physical literature "the k–leg watermelon". Each path of a watermelon along branches is a loop–erased random walk (LERW). Schematically, the k–leg watermelon is depicted in Fig. 1. In our work, we are mostly interested in the asymptotic behavior of $W_k(r)$ for large separations (i.e. for $r \gg 1$).

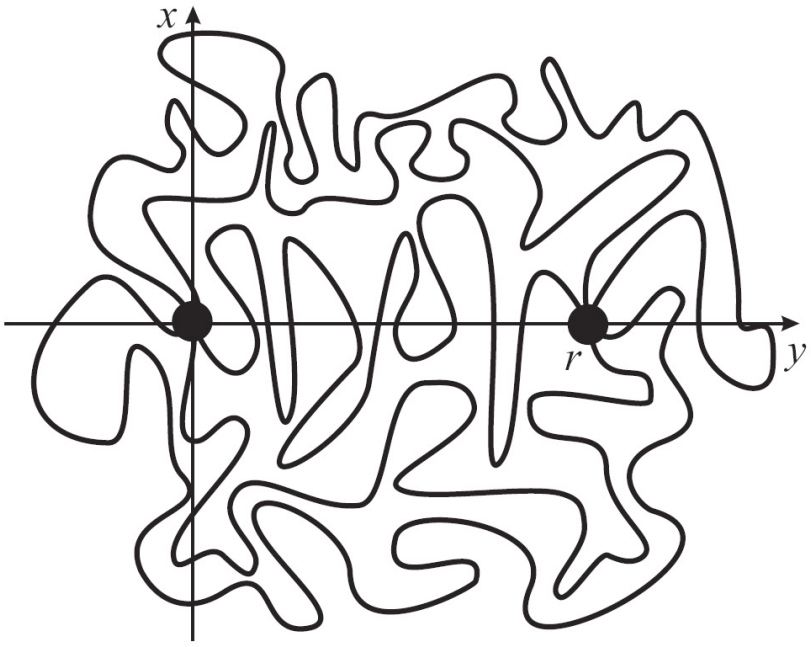

Figure 1: The example of 5-leg watermelon.

In the framework of the conformal field theory, the correlation function $W_k(r)$ of k connected clusters separated by the distance r and tied together at the extremities has

the following scaling behavior:

$$W_k(r) \sim r^{-2x_k} \tag{54}$$

where x_k is the conformal dimension of the scalar primary fields. By mapping to the q–state Potts model with arbitrary q one can see that each cluster of the Potts model in the limit $q \to 0$ contains a single path from one extremity to another. The values of scaling dimensions, $x_{p,q}$, have been computed as

$$x_{p,q} = 2h_{p,q}; \quad h_{p,q} = \frac{[(m+1)p - mq]^2 - 1}{4m(m+1)} \tag{55}$$

where $h_{p,q}$ are the weights belonging to the Kac table and p, q are integers in the minimal block, $1 \le p \le m-1$. The parameter m in (55) is fixed by the central charge c,

$$c = 1 - \frac{6}{m(m+1)} \tag{56}$$

For $c = -2$ (i.e., $m = 1$) one has

$$h_{p,q} = \frac{(2p-q)^2 - 1}{8} \tag{57}$$

and for $(p, q) = (k/2, 0)$ the large–distance scaling behavior of the k–path correlation function is

$$W_k(r) \sim r^{-4h_{k/2,0}} = r^{-\frac{k^2-1}{2}} \tag{58}$$

A combinatorial derivation of the exponent $\nu = (k^2-1)/2$ for the k–leg watermelon remains still an open problem. However, a "minor" modification of the problem makes it solvable. Instead of the k–leg watermelon embedded into the *single–component* spanning tree, one may consider the *two–component* spanning tree and put the watermelon into one of these components. Then, for sufficiently large components, the partition function of a k–leg watermelon for odd k is given by the determinant of the $k \times k$ matrix whose entries are the Green functions, Δ^{-1}, of the discrete Laplacian, Δ.

The partition function of the 3–leg watermelon embedded into the two–component spanning tree was computed for the first time in [3], where the 3–leg watermelon, called the θ–graph, was used for exact determination of the height probabilities in the Abelian sandpile model [4, 5]. The k–leg generalization of the θ–graph was the subject of [10], where the authors derived a determinant expression for the k–leg watermelon also embedded into one component of the two–component spanning tree. Calculating $W_k(r)$ for a few small values of k ($k = 1, 3, 5$) and guessing the structure of the series expansion of $W_k(r)$ at $r \gg 1$, the authors of [10] suggested the generic expression

$$W_k(r) \sim r^{-\frac{k^2-1}{2}} \ln r \tag{59}$$

where the logarithmic factor comes from the two–component topology of the problem (see e.g. [11]). Exact derivation of (59) needs more careful analysis. Below we show how the asymptotic correlation function (59) can be derived exactly from the corresponding determinant expression.

Watermelons of loop–erased random walks. Consider a finite square lattice $\mathcal{L}$ with the vertex set V and the edge set E. Select a tagged subset W ($W \subset V$) called "the set of dissipative vertices". Let $\mathcal{P} = [u_0, u_1, u_2, \ldots, u_n]$ be a collection of vertices (a trajectory) passed by an n–step random walk on $\mathcal{L}$, starting from u_0 and ending upon hitting $u_n \in W$. The loop–erasure $\mathrm{LE}(\mathcal{P}) = [\gamma_0, \gamma_1, \gamma_2, \ldots, \gamma_m]$ of $\mathcal{P}$ is defined by removing loops from $\mathcal{P}$ in a chronological order. Note that the order in which the loops are removed is important, and it is uniquely fixed by the condition that the loop is removed immediately as it is created when following the trajectory $\mathcal{P}$. The ordered collection of vertices $\mathrm{LE}(\mathcal{P})$ is called "the loop–erased random walk" (LERW) on $\mathcal{L}$ with the dissipation W.

Wilson [9] has proposed an algorithm to generate the ensemble of uniformly distributed spanning trees by LERWs. It turns out to be useful not only as a simulation tool, but also for a theoretical analysis. The algorithm runs as follows. Pick up an arbitrary ordering $V \setminus W = \{v_1, \ldots, v_N\}$ for the vertices in $\mathcal{L}$. Inductively, for $i = 1, 2, \ldots, N$ define a graph S_i ($S_0 = W$) which is a union of S_{i-1} and a (conditionally independent) LERW from v_i upon hitting S_{i-1}. If $v_i \in S_{i-1}$, then $S_i = S_{i-1}$. Regardless of the chosen order of the vertices, S_N is a sample of uniformly distributed (random) spanning forests on $\mathcal{L}$ with the set of roots, W. A spanning forest with a single root is a spanning tree. A spanning forest with a fixed set of roots can be considered as a spanning tree, if one adds an auxiliary vertex and join it to all the roots. If the size of the lattice tends to infinity, the boundary effects vanish, and one can neglect the details of the boundary. In what follows, we do not distinguish between spanning forests and spanning trees in this case, assuming all boundary vertices are connected to an auxiliary vertex.

Consider the set of k bulk vertices $I_k = \{i_1, i_2, \ldots, i_k\}$. The Wilson algorithm on $\mathcal{L}$ with the dissipation $W = \partial\mathcal{L} \cup I_k$ generates the $k+1$–component spanning forest with roots $i_1, i_2, \ldots, i_k$ and an auxiliary vertex connected to the boundary vertices. Given k, and introducing another set of k vertices, $J_k = \{j_1, j_2, \ldots, j_k\}$, we can enumerate all spanning forests, for which the vertices in J_k belong to the components with roots different from I_k (i.e. $I_k \cap J_k = 0$).

Construct now an auxiliary Laplacian on $\mathcal{L}$ using the bridge trick ([3]). Specifically, define the unperturbed Laplacian of the square lattice, Δ, and the perturbed Laplacian, Δ', which differs from Δ by "defects" (bridges) with the weights $-\eta$,

$$\Delta_{ij} = \begin{cases} 4 & \text{if } i = j \\ -1 & \text{if } i, j \text{ are nearest neighbors} \\ 0 & \text{otherwise} \end{cases}; \quad \Delta'_{ij} = \begin{cases} 4 & \text{if } i = j \\ -1 & \text{if } i, j \text{ are nearest neighbors} \\ -\eta & \text{if } i, j \text{ is a pair } (i_s, j_s),\ s = 1, ..., k \\ 0 & \text{otherwise} \end{cases} \tag{60}$$

One can check that the combination

$$\lim_{\eta \to \infty} \frac{1}{\eta^k} \det \Delta' \tag{61}$$

gives the sum over $k+1$–component spanning forests T having k bulk roots in the lattice points $I_k = \{i_1, i_2, \ldots, i_k\}$. Each forest T enters into the sum with the sign $(-1)^{c(T)}$,

where $c(T)$ is the number of cycles which appear in T due to adding bridges (i_s, j_s), $s = 1, 2, \ldots, k$ – see [3].

Following Ivashkevich and Hu [10], we chose the the sets I_k and J_k as zigzags (or "fences") with odd k – see Fig. 2a. Then, all possible configurations of cycles on the bridges contain either 1, or k cycles – see Fig. 3 and, therefore, $(-1)^{c(T)} = -1$. For fixed k and a large distance between the sets I_k and J_k, the bunch of lattice paths from J_k to I_k has the form of a watermelon. Connecting the neighboring points in the set I_k (and in the set J_k) we obtain a *two–component* spanning tree with the *watermelon embedded into one component*. Thus, we have

$$-\lim_{\eta\to\infty}\frac{1}{\eta^k}\det\Delta' = \text{number of } k\text{–leg watermelons} \tag{62}$$

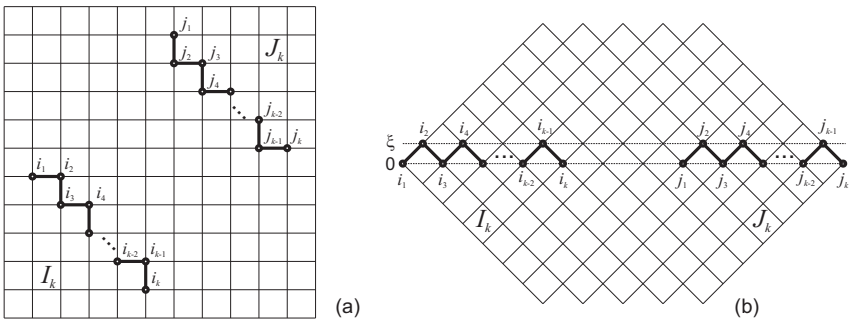

Figure 2: The k nonintersecting loop–erased random walks begin in the set I_k and end in the set J_k: (a) Sets I_k and J_k (k is odd)are chosen as parallel zigzags on the square lattice; (b) Sequential zigzags I_k and J_k are oriented along the horizontal axis.

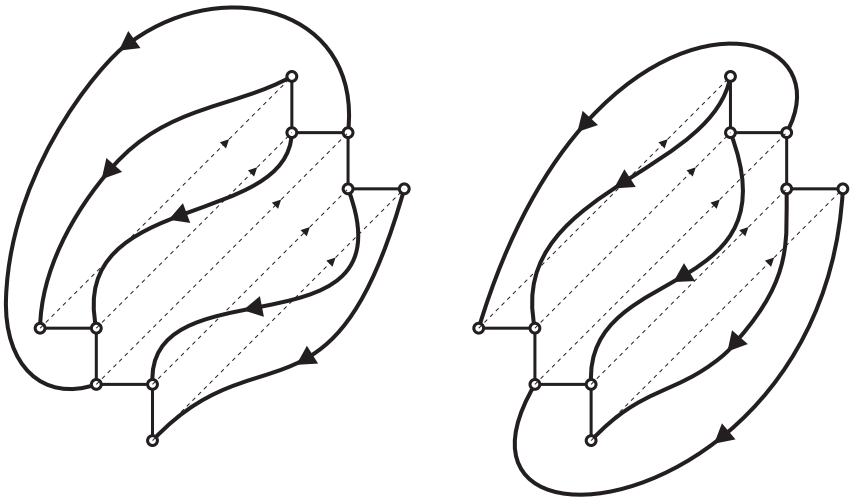

Figure 3: Possible closures of zigzags by loop–erased random walks.

The matrix Δ' can be represented as $\Delta' = \Delta + B$, where the matrix B has nonzero elements $-\eta$ for pairs (i_s, j_s), $s = 1, 2, \ldots, k$. To evaluate the determinant Δ', we use the

known formula [12]

$$\frac{\det \Delta'}{\det \Delta} = \det(\mathbb{I} + BG), \tag{63}$$

where $\mathbb{I}$ is the unit matrix, $G \equiv G(I_k, J_k)$ is the Green function $G = \Delta^{-1}$ of the bunch of lattice paths from the set I_k to the set J_k, and the nonzero part of the matrix B is the $k \times k$–matrix. Inserting (63) into (62) we obtain the ratio $W(I_k, J_k)$ between the number of two–component spanning trees containing the k–leg watermelon and the total number of spanning trees on lattice $\mathcal{L}$:

$$W(I_k, J_k) = \det G(I_k, J_k) \tag{64}$$

where the rows and columns of the matrix $G(I_k, J_k)$ are labelled by indices $i_1, i_2, \ldots, i_k$ and $j_1, j_2, \ldots, j_k$.

K-leg watermelon. The correlation function $W(I_k, J_k)$ at large separation, r, between the sets I_k and J_k (k is odd) takes an asymptotic form (see [10]):

$$W_k(r) \sim r^{-\nu} \ln r,$$

where ν is a universal lattice–independent exponent. To find ν, we have to specify the sets I_k and J_k on the square lattice and consider then the continuous limit $r \to \infty$. Following (64) we should define the matrix $G(I_k, J_k)$.

The Green function $G_{x,y}$ on a square lattice is the solution of the equation

$$-\frac{1}{4}\Big(G_{x-1,y} + G_{x,y-1} + G_{x+1,y} + G_{x,y+1}\Big) + G_{x,y} = \delta_{x,0}\delta_{y,0} \tag{65}$$

The integral form of $G_{x,y}$ is

$$G_{x,y} = \frac{1}{8\pi^2} \int_{-\pi}^{\pi} d\alpha \int_{-\pi}^{\pi} d\beta \, \frac{\cos(\alpha x)\cos(\beta y)}{2 - (\cos\alpha + \cos\beta)}, \tag{66}$$

For a specific configuration of the initial and final points we can fix: $x = x(j_1) - x(i_1)$, $y = y(j_1) - y(i_1)$, where the pairs $(x(i_k), y(i_k))$, $(x(j_k), y(j_k))$ label the coordinates of the vertices i_k, j_k, in the sets I_k and J_k respectively. Define $r = \sqrt{x^2 + y^2}$. At $r = 0$ the Green function $G_{x,y}$ is singular, and at large distances, $r \gg 1$, the function $G_{x,y} = G(r)$ has the asymptotic form

$$G(r) = G(0) - \frac{1}{2\pi} \ln r - \frac{\gamma}{2\pi} - \frac{3\ln 2}{4\pi} + \ldots \tag{67}$$

where γ is the Euler constant.

Taking the sets of the initial (I_k) and final (J_k) points as zigzags depicted in Fig. 2a and fixing the coordinates of the left ends, $i_1 \in I_k$ and $j_1 \in J_k$ as $x(i_1) = 0, y(i_1) = 0$ and $x(j_1) = x, y(j_1) = y$, we can easily define the coordinates of the vertices m in the zigzags I_k and J_k. So we have

$$\begin{aligned} x(i_m) &= \frac{m}{2}, & y(i_m) &= -\frac{m-2}{2} \\ x(j_m) &= x + \frac{m-2}{2}, & y(j_m) &= y - \frac{m}{2} \end{aligned} \tag{68}$$

for m even, and

$$\begin{aligned} x(i_m) &= \frac{m-1}{2}, & y(i_m) &= -\frac{m-1}{2} \\ x(j_m) &= x + \frac{m-1}{2}, & y(j_m) &= y - \frac{m-1}{2} \end{aligned} \tag{69}$$

for m odd.

Now we can explicitly write the expression for the determinant $W(I_k, J_k) = \det G(I_k, J_k)$ in (64) for a specific position of zigzags I_k and J_k (k is odd) shown in Fig. 2:

$$W(I_k, J_k) = \det \begin{pmatrix} G_{x,y} & G_{x,y-1} & G_{x+1,y-1} & G_{x+1,y-2} & \cdots & G_{x+k,y-k} \\ G_{x-1,y} & G_{x-1,y-1} & G_{x,y-1} & G_{x,y-2} & \cdots & \\ G_{x-1,y+1} & G_{x-1,y} & G_{x,y} & G_{x,y-1} & \cdots & \\ G_{x-2,y+1} & G_{x-2,y} & G_{x-1,y} & G_{x-1,y-1} & \cdots & \\ \vdots & \vdots & \vdots & \vdots & \ddots & \\ G_{x-k,y+k} & & & & & G_{x,y} \end{pmatrix} \tag{70}$$

The generic form of the entry in the position (m', m) of the matrix in (70) is $G_{x_{m,m'}, y_{m,m'}}$, where $x_{m,m'} = x(j_m) - x(i_{m'})$, $y_{m,m'} = y(j_m) - y(i_{m'})$, $\{m, m'\} = 1, \ldots, k$.

The explicit expression (70) allows one to extract the exponent ν for small $k = 1, 3, 5, \ldots$. However, the very origin of the general expression $\nu = (k^2 - 1)/2$ remains still hidden. To reveal it, note that the bridge construction used in the watermelon definition does not depend on the relative orientation of the sets I_k and J_k. Thus, we can choose a more convenient orientation shown in Fig.2b. To make a round along bridges possible, in the latter case we should insert bridges (i_s, j_{k+1-s}), $s = 1, 2, \ldots, k$ instead of the former ones (i_s, j_s), $s = 1, 2, \ldots, k$.

The asymptotic analysis of Eq.(64) does not need exact locations of the points $i_1, \ldots, i_k$ and $j_1, \ldots, j_k$ in the sites of the square lattice. Instead, we can choose for $i_1, \ldots, i_k$ and $j_1, \ldots, j_k$ two sets of the horizontal coordinates $0 \le u_1 < u_2 < \ldots, u_k <$ const and $r + v_1 < r + v_2 < \ldots < r + v_k$ with $0 \le v_i \le const$, $i = 1, \ldots, k$. The vertical coordinates of the points $i_1, \ldots, i_k$ and $j_1, \ldots, j_k$ will be 0 for odd indices and $\xi > 0$ for even ones. Given coordinates $\{u_i\}$ and $\{v_i\}$, the r–dependent part of the determinant in

(64) has the asymptotic form

$$\begin{vmatrix} \ln[(r-u_1+v_1)^2] & \ln[\xi^2+(r-u_2+v_1)^2] & \ln[(r-u_3+v_1)^2] & \cdots & \ln[(r-u_k+v_1)^2] \\ \ln[\xi^2+(r-u_1+v_2)^2] & \ln[(r-u_2+v_2)^2] & \ln[(\xi^2+(r-u_2+v_2)^2] & \cdots & \\ \ln[(r-u_1+v_3)^2] & \ln[\xi^2+(r-u_2+v_3)^2] & \ln[(r-u_2+v_2)^2] & \cdots & \\ \vdots & \vdots & \vdots & \ddots & \\ \ln[(r-u_1+v_k)^2] & & & & \ln[(r-u_k+v_k)^2] \end{vmatrix} \tag{71}$$

The matrix elements in Eq.(71) are of two types: $\ln[(r-u_i+v_j)^2]$ for odd–odd and even–even indices i and j and $\ln[\xi^2+(r-u_i+v_j)^2]$ for even–odd and odd–even indices. For a large distance r, we have $r \gg u_i$, $r \gg v_i, i = 1, \ldots, k$ and $r \gg \xi$. We rewrite the matrix elements as $2\ln r + 2\ln[1-u_i/r+v_j/r]$ and $2\ln r + \ln[(\xi/r)^2+(1-u_i/r+v_j/r)^2]$ and expand in powers of ξ/r, u_i/r and v_i/r.

Consider first the case $\xi = 0$. The leading term of the expansion of the determinant (71) is a totally antisymmetric polynomial of the form

$$\prod_{j>i}^{k}(u_i-u_j)\prod_{j>i}^{k}(v_i-v_j) \tag{72}$$

Each u_i and v_i brings the factor $1/r$, so that the leading term of the expansion is of an order of $r^{-k(k-1)}$ ln r.

Consider now the case $\xi > 0$. The sets I_k and J_k split into two subsets each, having vertical coordinates $\xi = 0$ and $\xi > 0$, respectively. To distinguish between different subsets, we supply the coordinates u_i and v_i for even i with hats: $\hat{u_i}$ and $\hat{v_i}$ and re-enumerate each subset in increasing order. We obtain four sets: $I_{n_1} = \{u_1, u_2, \ldots, u_{n_1}\}$, $I_{n_2} = \{\hat{u_1}, \hat{u_2}, \ldots, \hat{u_{n_2}}\}$,$J_{n_1} = \{v_1, v_2, \ldots, v_{n_1}\}$, and $J_{n_2} = \{\hat{v_1}, \hat{v_2}, \ldots, \hat{v_{n_2}}\}$, where $n_1 = (k+1)/2$ and $n_2 = (k-1)/2$. The resulting determinant is a totally antisymmetric function with respect to arguments $u_1, u_2, \ldots, u_{n_1}$, $\hat{u_1}, \hat{u_2}, \ldots, \hat{u_{n_2}}$, $v_1, v_2, \ldots, v_{n_1}$ and $\hat{v_1}, \hat{v_2}, \ldots, \hat{v_{n_2}}$ separately. Therefore, the first survived term in the expansion of the determinant has the form

$$\prod_{j>i}^{n_1}(u_i-u_j)\prod_{j>i}^{n_1}(v_i-v_j)\prod_{j>i}^{n_2}(\hat{u_i}-\hat{u_j})\prod_{j>i}^{n_2}(\hat{v_i}-\hat{v_j}) \tag{73}$$

and the contribution from $u, \hat{u}, v, \hat{v}$ to the leading term of the expansion is of an order of $r^{-\mu}\ln r$, where

$$\mu = n_1(n_1-1)+n_2(n_2-1) = \frac{k^2}{2}-k+\frac{1}{2} \tag{74}$$

Besides the horizontal coordinates $u, \hat{u}, v, \hat{v}$, we have to take into account the vertical coordinate ξ. The minimal order of ξ in the expansion of the determinant is $2n_2 = k-1$. Indeed, assume that the order of ξ is less than $2n_2$. It means that at least one row or

column of the matrix (71) is free of ξ, and as consequence, at least one element of the set I_{n_2} or J_{n_2} should be transferred to I_{n_1} or J_{n_1}. Then, we obtain instead of (74)

$$\mu' = \frac{n_1(n_1-1)}{2} + \frac{n_2(n_2-1)}{2} + \frac{n_1(n_1+1)}{2} + \frac{(n_2-2)(n_2-1)}{2} = \frac{k^2}{2} - k + \frac{5}{2} > \mu \quad (75)$$

Therefore, the minimal order of ξ is $k-1$ and the resulting exponent in the expansion of the determinant is

$$\nu = \mu + k - 1 = \frac{k^2-1}{2} \quad (76)$$

The sets I_k and J_k are the particular cases of more general sets $\tilde{I}_k = I_{n_1} \cup I_{n_2}$ and $\tilde{J}_k = J_{n_1} \cup J_{n_2}$, so the exponent in (59) coincides with ν.

Notes on the logarithmic conformal field theory. The logarithmic factor in (59) deserves a separate discussion. Let us begin with probabilistic and geometrical interpretations of the lattice Green function, $G = \Delta^{-1}$. Consider a connected graph, Γ, with a vertex set, V, edge set, E, and the Laplacian, Δ, defined on Γ. The infinite random walk on Γ is the set of vertices out of V, $v_0, v_1, v_2, \ldots, v_n, \ldots$, such that v_n and v_{n+1} are endpoints of an edge belonging to E. The vertex, v_0, is the starting point of the random walk. The Green function, $G_{x,y}$, can be defined as the expectation of visits of a vertex, $y \in V$, by the random walk starting at a vertex, $x \in V$. In contrast to this probabilistic interpretation, one can ascribe to G a purely geometric meaning. It is based on the proposition proved in [11].

Proposition. For an arbitrarily connected graph Γ with a fixed vertex v^* the Green function $G_{x,y}$ can be defined as

$$G_{x,y} = \frac{N^{(x,y)}}{N^{\rm tot}} \quad (77)$$

where $N^{(x,y)}$ is the number of two–rooted spanning trees with the roots v^* and y such that both vertices x and y belong to the same one-rooted subtree, and $N^{\rm tot}$ is the total number of spanning trees on Γ.

From the asymptotic form (67) of the Green function for the two–dimensional square lattice, we see that the logarithmic behavior of G can be associated with the connectivity condition between the vertices x and y inside the two–component spanning tree.

The auxiliary Laplacian (60) used for the bridge construction corresponds to a $k+1$-component spanning forest having k bulk roots in the vertex set, $I_k = \{i_1, i_2, \ldots, i_k\}$. Connecting sequentially the vertices I_k we get two–component spanning trees containing the k–leg watermelon inside one of the components. The ratio, $W(I_k, J_k)$, of the number of these components to the total number of spanning trees, is given by the determinant expression (64) which contains $k \times k$ Green functions. The asymptotic value of $W(I_k, J_k)$ is proportional to a single logarithm due to antisymmetry of the determinant. On the other hand, the bridge construction ensures k–path connectivity between two groups of vertices I_k and J_k belonging to the same component. So we can again associate the logarithmic behavior with the two–component geometry of clusters.

The geometrical interpretation of the Green functions is useful when one considers a correspondence between operators of the logarithmic conformal field theory (LCFT) and

characteristics of lattice models. The well-known example is the Abelian sandpile model [4, 5] where four height variables h_1, h_2, h_3, h_4 are expressed via spanning tree configurations [3]. In particular, heights h_2, h_3 and h_4 are represented by different combinations of the three–leg watermelons (θ–graphs). The description of heights by scaling fields was analyzed in [18]. It was shown that h_1 is a primary field with a conformal weight $(1, 1)$, while h_2, h_3 and h_4 are related to a field which can be identified with the logarithmic partner of h_1. This correspondence justifies the LCFT approach for the evaluation of the correlation functions $\langle h_1(x)h_i(y)\rangle$, $i = 2, 3, 4$ containing the logarithmic factor in the leading asymptotics. The predictions of the LCFT for $\langle h_1(x)h_i(y)\rangle$ were confirmed by direct lattice calculations [19].

It is interesting to note that the LCFT calculations for other correlators, like $\langle h_i(x)h_j(y)\rangle$, $i > 1$, $j > 1$ give the leading asymptotics $|x - y|^{-4} \log^2 |x - y|$. A geometric interpretation of the factor $\log^2(x)$ remains still an open problem.

It is instructive to compare the appearance of the logarithmic factor in the spanning tree model (i.e. $c = -2$ LCFT) with that in the percolation model (i.e. $c = 0$ LCFT) considered in [20]. For the percolation model on a torus, the authors of [20] defined a four–point correlation function, where two nearest–neighbor vertices i_1 and $i_1 + 1$ are separated by a distance r from other nearest–neighbor vertices i_2 and $i_2 + 1$. They defined: i) $P_{\neq}$ – a probability that two neighboring vertices belong to different Fortuin–Kasteleyn clusters, ii) $P_0(r)$ – a probability that all four vertices belong to different clusters, and iii) $P_1(r)$ – a probability that $i_1, i_1 + 1, i_2, i_2 + 1$ belong to three different clusters of which one "propagating" cluster contains i_1 or $i_1 + 1$ and i_2 or $i_2 + 1$. It was shown in [20] that the combination $P_0(r) + P_1(r) - P_{\neq}^2$ contains the logarithmic factor at the leading asymptotics $r^{-5/2}$. Like the spanning tree model, one can detect a role of cluster spanning the correlation distance r for the logarithmic contribution. However, the principal difference between the spanning tree model and the percolation deals with *the environment of the propagating cluster*. In the percolation model, this environment is an "archipelago" of the Fortuin–Kasteleyn clusters, properly distributed at the critical point, while in the spanning tree model, it can be associated with one connected cluster supplementary to the second component containing the watermelon.

A closely related problem of the LCFT is the existence of the Jordan cell in the transfer matrix formulation of the underlying lattice model. Bearing in mind the Temperley bijection [14] between dimer coverings and spanning trees, one would expect that the transfer matrix of the dimer model does contain the Jordan cells. However, it is not the case. Indeed, the transfer matrix of the dimer model on the two–dimensional square lattice derived by Lieb [24] is fully diagonalizable. It means that, to see a Jordan cell, we should decorate dimer configurations by an additional parameter which is hidden in the Lieb transfer matrix. For instance, given a spanning forest on the strip generated by a dimer configuration, one can ascribe numbers $1, \ldots, k$ to k trees rooted at the bottom row of the strip and follow this numeration in the course of the successive action of the transfer matrix. Each new branch of a tree gains the number of tree to which it is attached. The numeration imposes some restrictions on parity of branches of a given number oriented up or down at each row of the strip. Simple examples for small k show that the extended transfer matrix for the numbered trees contains the Jordan cell.

Another approach to the problem of Jordan cell was proposed by Pearce and Rasmussen [25] who considered the two–dimensional model of critical dense polymers. This model follows from the Temperley–Lieb algebra applied to the dense $O(n)$ loop model in the limit $n \to 0$. The model admits a mapping onto the spanning tree model with topologically non-trivial boundary conditions. The authors in [25] constructed the transfer matrix containing the Jordan cell for a narrow strip of width $N = 2, 4, 6, 8$ and conjectured that this property persists for $N \to \infty$.

The dense $O(n)$ loop model for $n = 1$ is equivalent to the percolation problem [23]. An identification of the Jordan cell for this case was considered in [21] (see also [22]). In the geometrical representation of the Temperley-Lieb algebra both the Hamiltonian and the transfer matrix are diagonalizable. However, one can introduce an additional parameter in one of the generators of the algebra, thereby deforming the original percolation model. The parameter labels the parity of contracted lines converting the structure of representation into that expected for the XXZ chain and contained in the Jordan cell.

[1] G. Kirchhoff, Ann. Phys. Chem. **72**, 497 (1847).

[2] H.Saleur and B. Duplantier, Phys. Rev. Lett. **58**, 2325 (1987).

[3] V.B. Priezzhev, J. Stat. Phys. **74**,955 (1994).

[4] P.Bak, C. Tang, and K. Wiesenfeld, Phys. Rev. Lett. **59**, 381 (1987).

[5] D.Dhar, Phys. Rev. Lett. **64**, 1613 (1990).

[6] M.E.Fisher, J. Stat. Phys. **34**, 667 (1984).

[7] D.A.Huse and M.E. Fisher, Phys. Rev. B **29**, 239 (1984).

[8] G.F. Lawler, O. Shram, and W. Werner, Ann. Probab. **32**, 939 (2004)

[9] J. G. Propp and D.B. Wilson, J. of Algorithms, **27**, 170 (1998).

[10] E.V. Ivashkevich and Chin-Kun Hu, Phys. Rev. E **71**, 015104 (R) (2005).

[11] E.V. Ivashkevich, D.V. Ktitarev, and V.B. Priezzhev, J. Phys. A: Math. Gen. **27**, L585 (1994).

[12] S.N. Majumdar and D. Dhar, J. Phys. A: Math. Gen. **24**, L357 (1991).

[13] S. Karlin and J. McGregor, Pacific J. Math. **9**, 1141 (1959).

[14] H.N.V. Temperley, in *Combinatorics: Proceedings of the British Combinatorial Conference*, London Mathematical Society Lecture Notes Series No. 13 Cambridge University Press, Cambridge, 202 (1974).

[15] V.B. Priezzhev, Soviet Physics Uspekhi **28**, 1125 (1985).

[16] J.F. Nagle, Phys. Rev. Lett. **34**, 1150 (1975).

[17] F. J. Dyson, J. Math. Phys. **3**, 1191 (1962).

[18] G. Piroux and P. Ruelle, Phys. Lett. B **607**, 188 (2005).

[19] V.S. Poghosyan, S.Y. Grigorev, V.B. Priezzhev, and P. Ruelle, J. Stat. Mech. P07025 (2010).

[20] R.Vasseur, J.L. Jacobsen, and H. Saleur, J. Stat. Mech. P07001 (2012).

[21] J.Dubail, J.L.Jacobsen and H.Saleur, Nucl. Phys. B 834, 399 (2010).

[22] R.Vasseur, J.L.Jacobsen and H.Saleur, Nucl. Phys B 851, 314 (2011).

[23] H.W.J. Blöte and B.Nienhuis, J.Phys. A 22, no. 9, 1415 (1989).

[24] E.H. Lieb, J. Math. Phys. **8** 2339 (1967).

[25] P.A. Pearce and J.Rasmussen, J. Stat. Mech. P02015 (2007).

CALCULATION OF THE PLASMA FREQUENCY OF A STACK OF COUPLED JOSEPHSON JUNCTIONS IRRADIATED WITH ELECTROMAGNETIC WAVES

Yu. M. Shukrinov [a,b], I. R. Rahmonov [a,c], and M. A. Gaafar [a,d]
[a] BLTP, JINR, Dubna, Moscow Region, 141980, Russia
[b] Max-Planck-Institute for the Physics of Complex Systems, 01187 Dresden, Germany
[c]Umarov Physical Technical Institute, TAS, Dushanbe, 734063 Tajikistan
[d]Department of Physics, Faculty of Science, Menoufiya University, Egypt.

Can superconducting layers in high temperature superconductors (HTSC) be charged? And if so, how would this be reflected in the properties of these materials? How strong is the influence of nonequilibrium effects on the physics of the intrinsic Josephson junctions in HTSC? These questions are very important for understanding the fundamental properties of superconductors[1, 2, 3, 4, 5, 6, 7] and radiation from the intrinsic Josephson junctions (JJ), naturally formed by a system of superconducting layers in HTSC such as $Bi_2Sr_2CaCu_2O_{8+\delta}$ (Bi-2122).[8]

In the present report based on the published paper [9] we give some answers to these questions. We perform a precise numerical study of phase dynamics in high temperature superconductors under electromagnetic radiation. A charging of superconducting layers in the bias current interval corresponding to the Shapiro step are found. We demonstrate a remarkable change in the longitudinal plasma wavelength at parametric resonance. Double resonance of the Josephson oscillations with radiation and plasma frequencies leads to additional parametric resonances and the non-Bessel Shapiro step.

There is no consensus about the mechanism of the terahertz radiation from these materials, which makes their investigation of great relevance today.[10] To make this situation clear, one needs a detailed and precise numerical study of their phase dynamics because the electrical and magnetic properties of intrinsic JJ in HTSC are strongly nonlinear.[10, 11, 12, 13, 14, 15]

One of the most spectacular indications of the Josephson effect in HTSC is a locking of the Josephson oscillations of each junction to the frequency of external electromagnetic radiation. This locking leads to the appearance of steps in the current voltage characteristics (IV-characteristics) at quantized voltages, called the Shapiro steps.[16, 17] Devices based on this effect are widely used as voltage standards. Therefore, a detailed study of the Shapiro steps in the intrinsic Josephson junctions under different resonance conditions would open an interesting field of research with potential for different applications.

Another interesting feature of the intrinsic JJ is a longitudinal plasma wave propagating along the c axis.[18, 19] A system of superconducting layers in an anisotropic HTSC, which is characterized by the order parameter $\Delta_l(t) = |\Delta| \exp(i\theta_l(t))$ with the time dependent phase $\theta_l(t)$, comprises N Josephson junctions[8]. The thickness of superconducting layers (about ~ 3 Å) in an HTCS is comparable with the Debye length r_D of electric charge screening. Therefore, there is no complete screening of the charge in the separate layers, and the electric field induced in each JJ penetrates into the adjacent junctions. Thus, the electric neutrality of superconducting layers is dynamically broken and,

in the case of the ac Josephson effect, a capacitive coupling appears between the adjacent junctions[18]. The absence of complete screening of charge in the superconducting layer leads to the formation of a generalized scalar potential Φ_l of the layer, which is related to the charge density Q_l in the superconducting layer as follows[18, 20]: $Q_l = -\frac{1}{4\pi r_D^2}\Phi_l$. The existence of a relationship between the electric charge Q_l of the l-th layer and the generalized scalar potential Φ_l of this layer reflects a nonequilibrium nature of the ac Josephson effect in layered HTSC[20]. In this case, the diffusion contribution to the quasiparticle current arises due to the generalized scalar potential difference, which is taken into account in the capacitively coupled Josephson junction model with diffusion current (CCJJ+DC model[21]). At $\omega_J = 2\omega_{LPW}$ (ω_J and ω_{LPW} are the Josephson and longitudinal plasma wave frequencies, respectively) the parametric resonance is realized: the Josephson oscillations excite the longitudinal plasma wave. The charge in the superconducting layer at parametric resonance can have complex oscillations depending on the number of junctions in the stack, coupling and dissipation parameters and boundary conditions. Fourier analysis [22] of the temporal dependence of the charge in a superconducting layer shows different frequencies in spectrum, in particular, ω_{LPW}, ω_J, and their combinations. The IV-characteristics of the intrinsic JJ display a multiple branch structure[24, 25, 26, 23] and have a breakpoint related to the parametric resonance and a parametric resonance region in the outermost branch before transition to the inner branch. Novel features of coupled JJ are described in Refs.[27, 28, 29, 30]. External radiation essentially changes the physical picture of the coupled Josephson junctions. In particular, the conditions for double resonance $\omega = \omega_J = 2\omega_{LPW}$ can be realized, where ω is the radiation frequency.

To investigate the phase dynamics of the intrinsic JJ, we use the one-dimensional CCJJ+DC model with the gauge-invariant phase differences $\varphi_l(t)$ between S-layers l and $l+1$ in the presence of electromagnetic irradiation described by the system of equations:

$$\begin{cases} \dfrac{\partial \varphi_l}{\partial t} = V_l - \alpha(V_{l+1} + V_{l-1} - 2V_l) \\ \dfrac{\partial V_l}{\partial t} = I - \sin\varphi_l - \beta\dfrac{\partial \varphi_l}{\partial t} + A\sin\omega t + I_{noise} \end{cases} \tag{78}$$

where t is the dimensionless time normalized to the inverse plasma frequency ω_p^{-1}, $\omega_p = \sqrt{2eI_c/\hbar C}$, C is the capacitance of the junctions, $\beta = 1/\sqrt{\beta_c}$, β_c is the McCumber parameter, α gives the coupling between junctions[18], and A is the amplitude of the radiation. To find the IV-characteristics of the stack of the intrinsic JJ, we solve this system of nonlinear second-order differential equations (1) using the fourth order Runge-Kutta method. In our simulations we measure the voltage in units of $V_0 = \hbar\omega_p/(2e)$, the frequency in units of ω_p, the bias current I and the amplitude of radiation A in units of I_c. The details of the model and simulation procedure are presented in Ref. [26].

It is known that in the case of a single Josephson junction with an increase in the radiation amplitude A a hysteresis region decreases, i.e., it leads to the decrease of the critical current value and the increase of the return current I_R.[31] For a stack of coupled JJ the external radiation leads additionally to a series of novel effects related to the parametric resonance and the longitudinal plasma wave propagating along the c axis.[18, 19] We demonstrate below three effects with an increase in the amplitude

of radiation A: (i) the changing of longitudinal plasma wavelength; (ii) the additional resonances around the Shapiro step; (iii) the double resonance $\omega_J = \omega = 2\omega_{LPW}$.

1. Variation of longitudinal plasma wavelength

The equation for the Fourier component of the difference $\delta\varphi_l = \varphi_{l+1,l} - \varphi_{l,l-1}$ between neighbor junctions can be written in linear approximation in the form[24] $\ddot{\delta}_k + \beta(k)\dot{\delta}_k + \cos(\Omega(k)\tau)\delta_k = 0$, where $\tau = \omega_p(k)t$, $\omega_p(k) = \omega_p C$, $\beta(k) = \beta C$, $\Omega(k) = \Omega/C$ and $C = \sqrt{1 + 2\alpha(1 - \cos(k))}$. This equation demonstrates the parametric resonance with a change in the parameters $\beta(k)$ and $\Omega(k)$ leading to the excitation of a longitudinal plasma wave with $\omega_p(k) = \omega_p\sqrt{1 + 2\alpha(1 - \cos(k))}$.

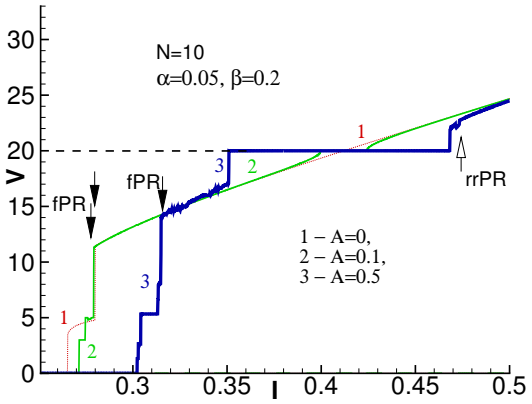

Figure 1: (Color online) The IV-characteristics of a stack with 10 coupled JJ without irradiation (curve 1) and under radiation with frequency $\omega = 2$ and amplitude $A = 0.1$ (curve 2) and amplitude $A = 0.5$ (curve 3). The filled arrows indicate the positions of the fundamental parametric resonance (fPR), while hollow arrow indicates the radiation related parametric resonance (rrPR).

First, we consider the case $\omega > 2\omega_{LPW}$ when the Shapiro step is above the parametric resonance region in IV-characteristics. Irradiation leads to the decrease of the hysteresis in the IV-characteristics[31, 22]. So it is expected that the parametric resonance point ($\omega_J = 2\omega_{LPW}$) would be shifted as well, and the longitudinal plasma wave frequency would increase. As far as we know, such a study was not carried out previously.

We investigate the influence of the external radiation on the parametric resonance by increasing the amplitude of the radiation at fixed frequency. Figure 1 shows three IV-characteristics of a stack with 10 coupled JJ: without irradiation (curve 1) and under radiation with $\omega = 2$, $A = 0.1$ (curve 2) and $A = 0.5$ (curve 3). At $\omega = 0$ the parametric resonance is characterized by the breakpoint current $I_{bp} \simeq 0.28$ and breakpoint voltage $V_{bp} \simeq 11.51$ corresponding to the Josephson frequency $\omega_J \simeq 1.151$[24]. The parametric resonance region in the IV-characteristics is shifted up along the voltage axis with increase in the amplitude of radiation. As we can see, the first Shapiro step is developed on the outermost branch of the IV-characteristics in the hysteresis region at $V = \omega_J N = 20$. The dashed line stresses this fact. The filled arrows indicate the positions corresponding to the

appearance of a fundamental parametric resonance in the stack, which is realized without radiation too. The hollow arrow indicates an additional parametric resonance before the Shapiro step that is caused by irradiation. We call this resonance a radiation related parametric resonance to distinguish it from the fundamental parametric resonance. We will discuss it below.

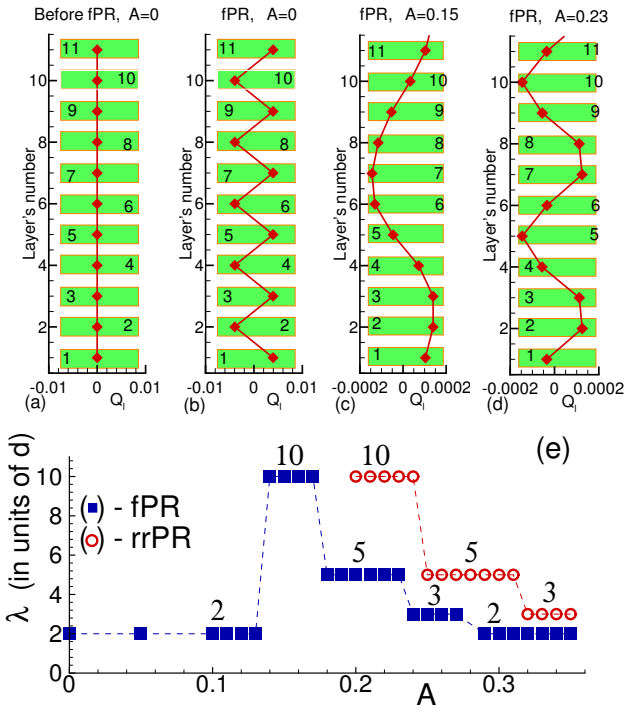

Figure 2: (Color online) Demonstration of the change in the wavelength of the longitudinal plasma mode at the fundamental parametric resonance with increase of the amplitude of radiation. The numbers count the layers in the stack. (a) $A = 0$, before resonance; (b) $A = 0$, at resonance ; (c) $A = 0.15$; (d) $A = 0.23$; (e) The longitudinal plasma wavelength at the fundamental parametric resonance (fPR) (filled squares) and radiation related parametric resonance (rrPR) (empty circles) in the amplitude interval $(0, 0.35)$ at $\omega = 2$.

We will now discuss the effect of the amplitude increase on the wavelength of the longitudinal plasma wave at the fundamental parametric resonance. Figure 2 demonstrates this effect at $\omega = 2$. We see that before the resonance region (Fig. 2a), the charge in the layers is zero (to within the noise level). In the growing region of the resonance (Fig. 2b) the amplitude of the charge oscillations increases exponentially forming the longitudinal plasma wave with the wave number $k = \pi$ ($\lambda = 2d$). At $A = 0.14$ *the wavelength of the created longitudinal plasma wave at the fundamental parametric resonance is changed by the external radiation.* The charge distribution along the stack, presented in Fig. 2(c), illustrates the wave with $\lambda = 10d$. At $A = 0.23$ we found that the wavelength of the LPW changed from $\lambda = 10d$ to $\lambda = 5d$, as shown in Fig. 2 (d).

The results of detailed investigations of the irradiation effects at $\omega = 2$ in the

amplitude range $(0, 0.35)$ are summarized in Fig. 2e which shows the variation of the longitudinal plasma wavelength with A. In the case of fundamental parametric resonance we register the following transitions of longitudinal plasma wave with increase in A: $\lambda = 2d \Rrightarrow \lambda = 10d \Rrightarrow \lambda = 5d \Rrightarrow \lambda = 3d \Rrightarrow \lambda = 2d$. An increase in A also changes the wavelength of the radiation related parametric resonance. In the case of the radiation related parametric resonance, as it demonstrated in Fig. 1, we observe the following transitions: $\lambda = 10d \Rrightarrow \lambda = 5d \Rrightarrow \lambda = 3d$ as A increases from zero to 0.35.

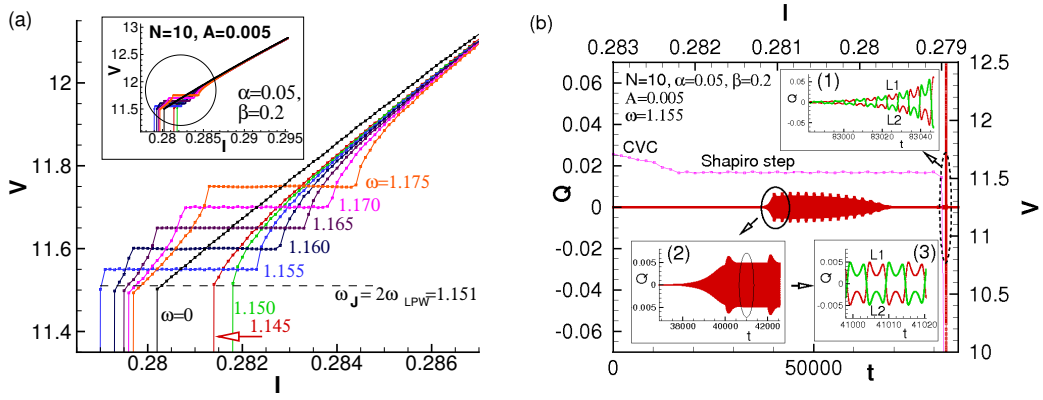

Figure 3: (Color online) (a) IV-characteristics of a stack with 10 coupled JJ under radiation with amplitude $A = 0.005$ and different frequencies. Thick curve (black online) shows IV-characteristics without irradiation. Inset stresses the coincidence of the curves before the Shapiro step; (b) Demonstration of the Shapiro step "charging". We show IV-characteristic with the Shapiro step (CVC, right and upper axes) together with a time dependence of the charge in superconducting layer. Inset (1) enlarges the charge oscillations in the parametric resonance region, insets (2) and (3) enlarge in consecutive order the charge oscillations in the Shapiro step region.

2. Double resonance in a system of coupled Josephson junctions

The double resonance condition $\omega_J = \omega = 2\omega_{LPW}$ can be approached by decreasing the radiation frequency: it produces the Shapiro step in the parametric resonance region. In Fig. 3a we show the IV-characteristics of a stack with 10 coupled JJ under radiation with the amplitude $A = 0.005$ and different frequencies. The numbers near the corresponding curves indicate the value of external radiation frequency. The thick curve (black online) shows the IV-characteristics without irradiation, while the inset stresses the coincidence of all curves before the Shapiro step. The Shapiro step does not appear at a frequency smaller than $\omega = 1.151$, because before it a jump to another branch occurs.

The double resonance demonstrates an interesting feature of coupled JJs which is absent in the case of a single JJ: when the external frequency is close enough to the parametric resonance condition $\omega_J = 2\omega_{LPW}$, *charge oscillations appear in the S-layers in the current interval corresponding to the Shapiro step ("charging" of the Shapiro step).* In our case, such charging appears starting from $\omega \simeq 1.1555$, while for the fundamental

parametric resonance without radiation it is realized at a Josephson frequency of $\omega_J = 1.151$. The amplitude of oscillations and the current interval of charging ("width of charging") grow as the double resonance condition is approached. Figure 3b demonstrates the charging of the Shapiro step at $\omega = 1.155$. It shows IV-characteristic with the Shapiro step (the curve with symbols denoted as CVC, related to the right and upper axes) together with a time dependence of the charge in the first superconducting layer. The enlarged parts of the charge-time dependence are shown in consecutive order in the insets (2) and (3). In the inset (3) we clearly see that the charge oscillations in the S-layers correspond to the π-mode of clearly longitudinal plasma wave. The inset (1) enlarges the charge oscillations in the time interval, corresponding to the bias current close to the transition to the inner branch and demonstrates that the fundamental parametric resonance survives at these radiation parameters. It also corresponds to the creation of the π-mode of the longitudinal plasma wave. However, of course, there are no restrictions on the creation of longitudinal plasma waves with other wave numbers at different parameters of the system and different radiation.

In summary, the nonequilibrium situation in the thin superconducting layers of HTSC, plays an important role in the variety of novel phenomena in the system of Josephson junctions naturally formed in these materials, related to their interaction with external radiation. Our detailed numerical study of the phase dynamics in the presence of radiation, revealed a series of effects specific to the coupled Josephson junctions and absent in the case of a single junction. We observed the charging of the superconducting layers in the bias current interval corresponding to the Shapiro step ("charging" Shapiro step). A remarkable change in the wavelength of the longitudinal plasma mode at the parametric resonance is important for understanding the fundamental properties of superconductors and radiation emitted from the intrinsic Josephson junctions. We expect that the double resonance of the Josephson oscillations with radiation and plasma frequencies demonstrating additional parametric resonances and the "non-Bessel" Shapiro step will be an object of intensive experimental investigations.

[1] V. M. Krasnov, Phys. Rev. Lett. **103**, 227002 (2009).

[2] A. M. Clark et al., Appl. Phys. Lett. **86**, 173508 (2005).

[3] Andrey V. Timofeev, Meri Helle, Matthias Meschke, Mikko Mottonen, and Jukka P. Pekola, Phys. Rev. Lett. 102, 200801 (2009).

[4] V. L. Ginzburg, Usp. Fiz. Nauk **174**, 1240 (2004).

[5] R. Barends, J. J. A. Baselmans, S. J. C. Yates, J. R. Gao, J. N. Hovenier, and T. M. Klapwijk, Phys. Rev. Lett. **100**, 257002 (2008).

[6] H. Matsumoto, S. Sakamoto, F. Wajima, T. Koyama, and M. Machida, Phys. Rev. B **60**, 3666 (1999).

[7] K. Kusakabe, J. Phys. Soc. Jpn. **78**, 114716 (2009).

[8] R. Kleiner, F. Steinmeyer, G. Kunkel, and P. Muller, Phys. Rev. Lett. **68**, 2394 (1992).

[9] Yu. M. Shukrinov, I. R. Rahmonov, M. A. Gaafar, Phys. Rev. B, **86**, 184502 (2012)

[10] Manabu Tsujimoto, Takashi Yamamoto, Kaveh Delfanazari, Ryo Nakayama, Takeo Kitamura, Masashi Sawamura, Takanari Kashiwagi, Hidetoshi Minami, Masashi Tachiki, Kazuo Kadowaki, and Richard A. Klemm, Phys. Rev. Lett. **108**, 107006 (2012).

[11] T. M. Benseman, A. E. Koshelev, K. E. Gray, W.-K. Kwok, U. Welp, K. Kadowaki, M. Tachiki, and T. Yamamoto, Phys. Rev. B **84**, 064523 (2011).

[12] V. M. Krasnov, Phys. Rev. B **83**, 174517 (2011).

[13] H. B. Wang, S. Guenon, B. Gross, J. Yuan, Z. G. Jiang, Y. Y. Zhong, M. Grunzweig, A. Iishi, P. H. Wu, T. Hatano, D. Koelle, and R. Kleiner, Phys. Rev. Lett. **105**, 057002 (2010).

[14] M. Tachiki, S. Fukuya, and T. Koyama, Phys. Rev. Lett. **102**, 127002 (2009).

[15] 1L. Ozyuzer, A. E. Koshelev, C. Kurter, N. Gopalsami, Q. Li, M. Tachiki, K. Kadowaki, T.Yamamoto, H. Minami,H.Yamaguchi, T. Tachiki, K. E. Gray, W.-K. Kwok, and U. Welp, Science **318**, 1291 (2007).

[16] S. Shapiro, Phys. Rev. Lett. **11**, 80 (1963)

[17] M. Tinkham, Introduction to Superconductivity, 2nd edition, McGraw-Hill, New York (1996)

[18] T. Koyama and M. Tachiki, Phys. Rev. B **54**, 16183 (1996)

[19] R. Kleiner, T. Gaber, and G. Hechtfischer, Phys. Rev. B **62**, 4086 (2000)

[20] D. A. Ryndyk, Phys. Rev. Lett. **80**, 3376 (1998).

[21] Yu. M. Shukrinov, F. Mahfouzi, P. Seidel. Physica C **449**, 62 (2006).

[22] Yu. M. Shukrinov, F. Mahfouzi, M. Suzuki, Phys. Rev. B **78**, 134521 (2008).

[23] Yu. M. Shukrinov and M. A. Gaafar, Phys. Rev. B **84**, 094514 (2011).

[24] Yu. M. Shukrinov, F. Mahfouzi, Supercond. Sci. Technol., **19**, S38-S42 (2007).

[25] Yu. M. Shukrinov, F. Mahfouzi, Phys. Rev. Lett. **98**, 157001 (2007).

[26] Shukrinov, Yu., Mahfouzi, F., Pedersen, N.: Phys.Rev. B, **75**, 104508 (2007)

[27] Yu. M. Shukrinov, M. Hamdipour, M. R. Kolahchi, A. E. Botha, and M. Suzuki, Phys. Lett. A, **376**, 3609 (2012).

[28] Yu. M. Shukrinov, I. R. Rahmonov, K. Kulikov, JETP Letters, **96**, 657 (2012).

[29] Yu. M. Shukrinov, M. Hamdipour, JETP Letters, **95**, 336 (2012)

[30] Yu. M. Shukrinov and I. R. Rahmonov, **115**, 289 (2012)

[31] W. Buckel and R. Kleiner, *Superconductivity: Fundamentals and Applications* (Wiley-VCH, 2004).

MONOGRAPHS

1. R. Pincak, M. Pudlak, J. Smotlacha, "Electronic properties of single and double wall carbon nanotubes," in *Carbon Nanotubes:Synthesis, Properties and Applications (NOVA Science Publisher, NY, 2012).*

2. N.M. Plakida, "Projection operator method," in *Strongly Correlated Systems. Theoretical methods, edited by A. Avella and F. Mancini (Springer Series in Solid-State Sciences, Vol. 171, Springer-Verlag, Berlin, 2012) Chap. 6, pp. 173–202.*

JOURNAL PUBLICATIONS

1. B. L. Aneva, J. G. Brankov, "Algebraic approach to directed stochastic avalanches", *Theor. Math. Phys.* **169** *(2011) No. 3, 1751–1766.*

2. P.Kh. Atanasova, T.L. Boyadjiyev, Yu.M. Shukrinov, Ye.V. Zemlyanaya, "Numerical Modeling of Long Josephson Junctions in the Frame of the Sine.Gordon Double Equation," *Mathematical Models and Computer Simulations, (2011), Vol. 3, No. 3, pp. 388 - 397.*

3. P.Kh. Atanasova, E.V. Zemlyanaya, T.L. Boyadjiev, Yu.M. Shukrinov, "Numerical study of magnetic flux in the LJJ model with double sine-Gordon equation," *Lecture Notes in Computer Science, Springer, (2011), Vol.6046, 347-352.*

4. J.G. Brankov, N.S. Tonchev, "Generalized inequalities for the Bogoliubov – Duhamel inner product with applications in the Approximating Hamiltonian method," *Cond. Mat. Phys.* **14** *(2011) No. 1, 13003 (17 pp.).*

5. J.G. Brankov, N.S. Tonchev, "Lower and upper bounds on the fidelity susceptibility", *Phys. Rev. E* **85** *(2012) No. 3, 031115 (1–8).*

6. A.Yu. Cherny, E.M. Anitas, V.A. Osipov, and A.I. Kuklin, "Deterministic fractals: Extracting additional information from small-angle scattering data", *Phys. Rev. E* **84** *(2011) 036203 (1–11).*

7. A.Yu. Cherny, J.-S. Caux, J. Brand, "Theory of superfluidity and drag force in the one-dimensional Bose gas", *Front. Phys.* **7** *(2012) 54–71.*

8. A.Yu. Cherny, E.M. Anitas, V.A. Osipov, and A.I. Kuklin, "Small-angle scattering from generalized self-similar Vicsek fractals", *J. Phys.: Conf. Ser.* **351** *(2012) 012020 (1–8).*

9. A.Yu. Cherny, E.M. Anitas, V.A. Osipov, A.I. Kuklin, "A model of small-angle scattering from three-phase fractal systems", *J. Phys.: Conf. Ser.* **393** *(2012) 012031 (1–6).*

10. A.Yu. Cherny, E.M. Anitas, V.A. Osipov, A.I. Kuklin, "Prospects for investigating deterministic fractals: Extracting additional information from small-angle scattering data", *J. Phys.: Conf. Ser.* **393** *(2012) 012032 (1–2).*

11. A.V. Chizhov, R.G. Nazmitdinov, "Orbital entanglement in an exactly solvable two-electron quantum dot model," *J.Phys.: Conf. Ser. 343 (2012) 012023.*

12. A.V. Chizhov, "Entanglement of electron orbital motion in open two-electron quantum dots," *J. Phys.: Conf. Ser.* **393** *(2012) 012010.*

13. M.L. Craus, E.M. Anitas, N. Cornei, A. Islamov, V. Garamus, "Magnetic structure of $La_{0.54}Ho_{0.11}Sr_{0.35}Mn_{1-x}Cu_xO_3$ manganites," *Solid State Phenomena, 190 (2012) 121.*

14. A.E. Derbyshev, S.S. Poghosyan, A.M. Povolotsky, V.B. Priezzhev, "The totally asymmetric exclusion process with generalized update," *J. Stat. Mech., (2012) P05014.*

15. F.A.H. Dolan, V.P. Spiridonov, and G.S. Vartanov, "From $4d$ superconformal indices to $3d$ partition functions," *Phys. Lett.* **B704***, no. 3 (2011) 234-241.*

16. A. Ferraz, E.A. Kochetov "Effective action for strongly correlated electron systems," *Nuclear Physics B 853 (2012) 710.*

17. A. Ferraz, E.A. Kochetov "Comment on "Fermi surface reconstruction in hole-doped t-J models without long-range antiferromagnetic order", *Phys. Rev. B86 (2012) 247103.*

18. A. Ferraz, E.A. Kochetov "Comment on "Z_2-slave-spin theory for strongly correlated fermions," *Phys. Rev. B87 (2013) 037101.*

19. D. Gurevich, P. Pyatov, P. Saponov, "Braided differential operators on quantum algebras," *J. Geom. Phys.* **61** *(2011) 1485-1501.*

20. D. Gurevich, P. Pyatov, P. Saponov, "Braided Weyl algebras and differential calculus on $U(u(2))$," *J. Geom. Phys.* **62** *(2012) 1175-1188.*

21. A.S. Haupt, T.A. Ivanova, O. Lechtenfeld, and A.D. Popov, "Chern-Simons flows on Aloff-Wallach spaces and Spin(7)-instantons," *Phys. Rev. D* **83** *(2011) 105028.*

22. G.N. Hayrapetyan, E.Sh. Mamasakhlisov, Vl.V. Papoyan, S.S. Poghosyan "The melting phenomenon in random-walk model of DNA," *Physics of atomic nuclei* **75** *(2012) 1268-1271.*

23. G.N. Hayrapetyan, V.F. Morozov, V.V. Papoyan, S.S. Poghosyan, V.B. Priezzhev, "The helix-coil transition in a double-stranded polynucleotide and the two-dimensional Random walk, *Mod. Phys. Lett., v. 26, no. 13 (2012) 1250083.*

24. V. Ilkovič, "Magnetic reorientation in a ferrimagnetic monolayer", *phys. stat.sol. (b)* **249** *(2012) 181-184.*

25. V.I. Inozemtsev, "Factorization of wave functions of the quantum integrable particle systems," *Letters to Physics of Particles and Nuclei,* **8** *(2011) 262-265.*

26. N.G. Inozemtseva, V.I. Inozemtsev, P.N. Sysoev, "On Compton scattering on the target with degenerate states," *MSU Bulletin, Physics, No. 3 (2011) 115-117.*

27. V.I. Inozemtsev, P.N. Sysoev, "On the configurations of classical Yang-Mills fields with topological charge k=4," *MSU Bulletin, Physics, No.1 (2012) 65-68.*

28. T.A. Ivanova and A.D. Popov, "Instantons on special holonomy manifolds," *Phys. Rev. D* **85** *(2012) 105012.*

29. V.L. Katkov, O.G. Isaeva, V.A. Osipov, "Resonant Tunneling In Graphene-DNA-Base-Graphene Junctions," *J. Phys.: Conf. Ser. 393 (2012) 012026.*

30. D.V. Kolesnikov and V.A. Osipov, "Low-temperature thermal conductivity in polycrystalline graphene," *Europhys. Lett. 100 (2012) 26004.*

31. S.E. Krasavin, "Effect of Charged Dislocation Walls on Mobility in GaN Epitaxial Layers," *Semiconductors 46 (2012) 598.*

32. C. Krattenthaler, V.P. Spiridonov, and G.S. Vartanov, "Superconformal indices of three-dimensional theories related by mirror symmetry," *J. High Energy Phys.* **06** *(2011) 008.*

33. A.I. Kuklin, A.V. Rogachev, A.Yu. Cherny, E.B. Dokukin, A.Kh. Islamov, Yu.S. Kovalev, T.N. Murugova, D.V. Soloviev, O.I. Ivankov, A.G. Soloviev, V.I. Gordeliy, "Do the size effects exist?", *Rom. J. Phys.* **56** *(2011), No. 1-2, 134-140.*

34. A.L. Kuzemsky, "Electronic Transport in Metallic Systems and Generalized Kinetic Equations", *Intern. J. Mod. Phys. B* **25** *(2011) No. 23-24, 3071–3183.*

35. A.L. Kuzemsky, "Bogoliubov's Foresight and Development of the Modern Theoretical Physics", *Electronic J. Theor. Phys.* **8** *(2011) No. 25, 1–14.*

36. A.L. Kuzemsky, "Generalized Van Hove Formula for Scattering of Neutrons by the Nonequilibrium Statistical Medium", *Intern. J. Mod. Phys. B* **26** *(2012) No. 13, 1250092 (1–34).*

37. M.M. Maska, M. Mierzejewski, E.A. Kochetov, L. Vidmar, J. Bonca, O.P. Sushkov, "Effective approach to the Nagaoka regime of the two-dimensional t-J model," *Phys. Rev. B85 (2012) 245113.*

38. R.G. Nazmitdinov, A.V. Chizhov, "Quantum entanglement in a two-electrom quantum dot in magnetic field," *Optics and Spectroscopy 112 (2012) 319-322.*

39. R.G. Nazmitdinov, N.S. Simonovic, A.R. Plastino, A.V. Chizhov, "Shape transitions in excited states of two-electron quantum dots in a magnetic field," *J.Phys. B: Atomic, Molecular and Optical Physics 45 (2012) 205503(1)-205503(4).*

40. V.O. Nesterenko, A.N. Novikov, and E. Suraud, "Strong-coupling dynamics of Bose-Einstein condensate in a double-well trap," *J. Phys. B: At. Mol. Opt.Phys. 45 (2012) 225303.*

41. A.E. Patrick, "A Droplet Within the Spherical Model," *J. Stat. Phys.* **142** *(2011) 1085-1104.*

42. N.Ch. Pesheva, J.G. Brankov, "Position-induced phase change in a TASEP with a double-chain section (a model of biological transport)", *Biomath* **1** *(2012) No. 2, 121121 (1–7).*

43. R. Pincak, J. Smotlacha, and M. Pudlak, "Electronic properties of perturbed cylinder," *J. Phys.: Conf. Ser.* 393 (2012) 012029.

44. N. M. Plakida, "Comments on the paper "The pairing mechanism of high-temperature superconductivity: experimental constraints", *Phys. Scripta* **83** *(2011) 038303 (1–3).*

45. N. M. Plakida, "The two-time Green's function and the diagram technique", *Theor. Math. Phys.* **168** *(2011) No. 3, 1303–1317.*

46. S.S. Poghosyan, V.S. Poghosyan, V.B. Priezzhev, and P. Ruelle, "Numerical study of correspondence between the dissipative and fixed-energy Abelian sandpile models," *Phys. Rev. E 84 (2011) 066119.*

47. V.S. Poghosyan, V.B. Priezzhev, "The Problem of Predecessors on Spanning Trees," *Acta Polytechnica, Vol. 51, No. 1 (2011) 59-62.*

48. V.S. Poghosyan, V.B. Priezzhev and P. Ruelle, "Return probability for the loop-erased random walk and mean height in the Abelian sandpile model: a proof, *J. Stat. Mech. (2011) P10004.*

49. S.S. Poghosyan, A.M. Povolotsky, V.B. Priezzhev , "Universal exit probabilities in the TASEP," *J. Stat. Mech. (2012) P08013.*

50. A.M. Povolotsky, V.B. Priezzhev, and G.M. Schutz, "Generalized Green Function and Current Correlations in the TASEP, *J. Stat. Phys. v. 142 (2011) 754.*

51. A.M. Povolotsky, V.B. Priezzhev, "Multiparticle space-time transitions in the totally asymmetric simple exclusion process," *Theor. Math. Phys., v.169 (2011) 1507-1514.*

52. I.R. Rahmonov, Yu.M. Shukrinov, E.V. Zemlyanaya, I.Sarhadov and O. Andreeva, "Mathematical modeling of intrinsic Josephson junctions with capacitive and inductive couplings," *J.Phys.: Conf. Ser. 393 (2012) 012022.*

53. J.A. Seman, E.A. Henn, R.F. Shiozaki, G. Roati, F.J. Poveda-Cuevas, K.M. Magalhaes, V.I. Yukalov, M. Tsubota, M. Kobayashi, K. Kasamatsu, and V.S. Bagnato, "Route to turbulence in a trapped Bose-Einstein condensate", *Laser Phys. Lett.* **8** *(2011) 691–696.*

54. R.F. Shiozaki, G.D. Telles, V.I. Yukalov, and V.S. Bagnato, "Transition to quantum turbulence in finite-size superfluids", *Laser Phys. Lett.* **8** *(2011) 393–397.*

55. Yu.M. Shukrinov, I.R. Rahmonov, K. Kulikov, "Double Resonance in the system of coupled Josephson Junctions," *JETP Letters 96 (2012) 588-595.*

56. Yu.M. Shukrinov, I.R. Rahmonov, M.A. Gaafar, "Calculation of the plasma frequency of a stack of coupled Josephson junctions irradiated with electromagnetic waves," *Phys.Rev. B86 (2012) 184502.*

57. Yu.M. Shukrinov and I.R. Rahmonov, "Diffusion Current in a System of Coupled Josephson Junctions," *JETP 115 (2012) 289-302.*

58. Yu.M. Shukrinov, P. Seidel, E. Ilichev, W. Nawrocki, M. Grajcar, P.A. Plecenik, I.R. Rahmonov, K. Kulikov, "Resonance Features of the Coupled Josephson Junctions: Radiation and Shunting," *J. Phys.: Conf. Ser. 393 (2012) 012020.*

59. Yu.M. Shukrinov and M.A. Gaafar, "Charging of superconducting layers and resonance-related hysteresis in the current-voltage characteristics of coupled Josephson junctions," *Phys. Rev. B84 (2011) 094514.*

60. Yu. Shukrinov and P. Seidel, "Resonance features of coupled Josephson junctions in high temperature superconductors," *Elektronika 6 (2011) 52-54.*

61. J. Smotlacha, R. Pincak, M. Pudlak, "Electronic structure of disordered graphene with Green's function approach," *Phys. Lett. A 376 (2012) 3256.*

62. J. Smotlacha, R. Pincak, M. Pudlak, "Electronic Structure of Disclinated Graphene in an Uniform Magnetic Field," *Eur.Phys.J. B84 (2011) 255-264.*

63. V.P. Spiridonov, "Elliptic beta integrals and solvable models of statistical mechanics," *Contemp. Math.* **563** *(2012) 181–211.*

64. V.P. Spiridonov and G.S. Vartanov, "Superconformal indices of $\mathcal{N} = 4$ SYM field theories," *Lett. Math. Phys.* **100** *(2012) 97–118.*

65. V.P. Spiridonov and G.S. Vartanov, "Elliptic hypergeometry of supersymmetric dualities," *Commun. Math. Phys.* **304** *(2011) 797–874.*

66. V.P. Spiridonov and G.S. Vartanov, "Elliptic hypergeometric integrals and 't Hooft anomaly matching conditions," *J. High Energy Phys.* **06** *(2012) 016.*

67. V.P. Spiridonov and S.O. Warnaar, "New multiple ${}_6\psi_6$ summation formulas and related conjectures," *Ramanujan J.* **25**, *no. 3 (2011) 319–342.*

68. V.P. Spiridonov, "Elliptic hypergeometric terms," *SMF Séminaire et Congrès* **23** *(2011) 385–405.*

69. A.A. Vladimirov, D. Ile, and N.M. Plakida, "Dynamic spin susceptibility of superconducting cuprates: A microscopic theory of the magnetic resonance mode, *Phys. Rev. B* **83** *(2011) 024411 (1–13).*

70. A.A. Vladimirov, D. Ihle, and N.M. Plakida, "Optical and dc conductivities of cuprates: Spin-fluctuation scattering in the t-J model", *Phys. Rev. B* **85** *(2012) 224536 (1–12).*

71. V.I. Yukalov, "Basics of Bose-Einstein condensation", *Phys. Part. Nucl.* **42** *(2011) 460–513.*

72. V.I. Yukalov, "Nonequilibrium representative ensembles for isolated quantum systems", *Phys. Lett. A* **375** *(2011) 2797–2801 .*

73. V.I. Yukalov, "Equilibration and thermalization in finite quantum systems", *Laser Phys. Lett.* **8** *(2011) 485–507.*

74. V.I. Yukalov and E.P. Yukalova, "Possibility of superradiance by magnetic nanoclusters", *Laser Phys. Lett.* **8** *(2011) 804–813.*

75. V.I. Yukalov, A. Rakhimov, and S. Mardonov, "Quasi-equilibrium mixture of itinerant and localized Bose atoms in optical lattice", *Laser Phys.* **21** *(2011) 264–270.*

76. V.I. Yukalov, E.P. Yukalova, "Mesoscopic disorder in double-well optical lattices", *Laser Phys.* **21** *(2011) 1448–1458.*

77. V. I. Yukalov, D. Sornette, "Decision theory with prospect interference and entanglement", *Theor. Dec.* **70** *(2011) 283–328.*

78. S. Gluzman, V.I. Yukalov, "Self-similar continued root approximants", *Phys. Lett. A* **377** *(2012) 124–128.*

79. V.I. Yukalov, D. Sornette, "Statistical outliers and dragon-kings as Bose-condensed droplets", *Eur. Phys. J. Spec. Top.* **205** *(2012) 53–64.*

80. V.I. Yukalov, E.P . Yukalova, D. Sornette, "Extreme events in population dynamics with functional carrying capacity", *Eur. Phys. J. Spec. Top.* **205** *(2012) 313–354.*

81. V.I. Yukalov, E.P. Yukalova, "Fast magnetization reversal of nanoclusters in resonator", *J. Appl. Phys.* **111** *(2012) No. 2, 023911 (1–9).*

82. V.I. Yukalov, E.P. Yukalova, "Statistics of multiscale fluctuations in macromolecular systems", *J. Phys. Chem. B* **116** *(2012) 8435–8448.*

83. V.I. Yukalov, E.P. Yukalova, "Coherent spin dynamics of nanomolecules and magnetic nanoclusters", *J. Phys.: Conf. Ser.* **393** *(2012) 012004 (1–9).*

84. V.I. Yukalov, E.P. Yukalova, "Double-well optical lattices with atomic vibrations and mesoscopic disorder", *Laser Phys.* **22** *(2012) 1070–1080.*

85. V.I. Yukalov, E.P. Yukalova, D. Sornette, "Modeling symbiosis by interactions through species carrying capacities", *Physica D: Nonlin. Phen.* **241** *(2012) 1270–1289.*

86. V.I. Yukalov, "Equilibration of quasi-isolated quantum systems", *Phys. Lett. A* **376** *(2012) No. 4, 550–554.*

87. V.I. Yukalov, "Decoherence and equilibration under nondestructive measurements", *Ann. Phys. (Elsevier)* **327** *(2012) No. 2, 253–263.*

88. V.I. Yukalov, "Difference in Bose-Einstein condensation of conserved and unconserved particles", *Laser Phys.* **22** *(2012) 1145–1168.*

89. P.E. Zhidkov, "On the radially symmetric solutions of the equation $-\Delta u + u = |u|^{p-1}u$. An ODE approach," *Ricerche di Matematica, Vol.* **61***, No 1 (2012) 125-137.*

ARTICLES ACCEPTED FOR PUBLICATIONS

1. A. Gorsky, S. Nechaev, V.S. Poghosyan, V.B. Priezzhev, "From elongated spanning trees to vicious random walks," *accepted in Nucl. Phys. B, arXiv:1206.3147.*

2. G.N. Hayrapetyan, Y.Sh. Mamasakhlisov, V.F. Morozov, Vl.V. Papoyan, and V.B. Priezzhev,"Two-dimensional random walk and critical behavior of double-strand DNA," *accepted in J.Phys. A: Math. and Theor.*

3. P.V. Kharebov, V.K. Henner, V.I. Yukalov, "Optimal conditions for magnetization reversal of nanocluster assemblies with random properties", *J. Appl. Phys.* **113** *(2013) 043902 (1–8).*

4. A.E. Patrick, "Large Deviations in the Spherical Model: The Rate Functions," *accepted in J. Stat. Phys., arXiv:1204.2223.*

5. N.S. Tonchev, J.G. Brankov, "Some inequalities in the fidelity approach to phase transitions", *J. Optoel. Adv. Mater. (2013) to appear.*

6. V.I. Yukalov, E.P. Yukalova, "Order indices of density matrices for finite systems", *Comput. Theor. Chem.* **1003** *(2013) 37–43.*

7. P.E. Zhidkov, "On weak solutions of the initial value problem for the equation $u_{tt} = a(x,t)u_{xx} + f(t,x,u,u_t,u_x)$," *accepted in Nonlinear Analysis: Theory, Methods and Applications.*

PREPRINTS AND DATA BASES

1. J.G. Brankov, N.S. Tonchev, "Lower and upper bounds on the fidelity susceptibility", *arXiv:1112.4184 (2011).*

2. A.E. Derbyshev, S.S. Poghosyan, A.M. Povolotsky, and V.B. Priezzhev, "The totally asymmetric exclusion process with generalized update," *arXiv:1203.0902.*

3. S.E. Derkachov and V.P. Spiridonov, "Yang-Baxter equation, parameter permutations, and the elliptic beta integral," *arXiv:1205.3520.*

4. A.L. Kuzemsky, "Statistical Mechanics and the Physics of Many-Particle Model Systems", *arXiv:1101.3423v1 (2011).*

5. A.L. Kuzemsky, "Bogoliubov's Vision: Quasiaverages and Broken Symmetry to Quantum Protectorate and Emergence", *arXiv:1110.1189v1 (2011).*

6. A.L. Kuzemsky, "Fundamental Principles of Theoretical Physics and Concepts of Quantum Protectorate and Emergence", *arXiv.org/abs/1203.3139 (2012).*

7. A.L. Kuzemsky, "To the Problem of the Intrinsic Magnetism in Carbon-Based Systems: pro et contra", *arXiv:1210.3687v1 [cond-mat.str-el] (2012).*

8. R.G. Nazmitdinov, A.V. Chizhov, " ", *JINR Preprint 17-2011-56.*

9. N.M. Plakida, V.S. Oudovenko, "On the theory of superconductivity in the extended Hubbard model: Spin-fluctuation pairing", *arXiv:13.014347[cond-mat.str-el] (2013) (17 pp.).*

10. S.S. Poghosyan, A.M. Povolotsky, and V.B. Priezzhev, "Universal exit probabilities in the TASEP," *arXiv:1206.3429.*

11. V.S. Poghosyan, V.B. Priezzhev, "Correlations in the $n \to 0$ limit of the dense O(n) loop model," *arXiv:1212.1032, submitted to J. Phys. A: Math. and Theor.*

12. Yu. M. Shukrinov, I.R. Rahmonov, M.A. Gaafar, "Variation of Longitudinal Plasma Wavelength under Irradiation and Double Resonance in Coupled Josephson Junctions," *Cond-Mat arXiv:1205.6923.*

13. V.P. Spiridonov, "Modified elliptic gamma functions and $6d$ superconformal indices," *arXiv:1211.2703.*

14. V.P. Spiridonov and G.S. Vartanov, "Elliptic hypergeometry of supersymmetric dualities II. Orthogonal groups, knots, and vortices," *arXiv:1107.5788.*

15. N.S. Tonchev, J.G. Brankov, "Some inequalities in the fidelity approach to phase transitions", *arXiv:1210.0364 (2012).*

CONFERENCE CONTRIBUTIONS

1. J.G. Brankov, "Position-induced phase change in a TASEP with a double-chain section (a model of biological transport)", *Intern. Scientific Conf. on Mechanics "MECH2012", Institute of Mechanics, Bulgarian Academy of Sciences, 19 - 22 November, Sofia, Bulgaria.*

2. A.V. Chizhov, R.G. Nazmitdinov, "Quantum entanglement of two-electron orbital motion in a quantum dot in a perpendicular magnetic field" (Optics-2011), *"Optics and its Applications: Symposium Information and Book of Abstracts of the International Symposium" (Armenia, 5-9 September, 2011), Yerevan, 2011, p.71.*

3. A.V. Chizhov, "Spatial-momentum quantum correlations in a two-electron quantum dot" *XLVIII All-Russian Conf. on Problems in Particle Physics, Plasma Physics, Condensed Matter, and Optoelectronics, May 15-18, 2012, RUDN, Moscow,pp. 89-90.*

4. V. Ilkovič, "Towards the theory of magnetic reorientation in the ferrimagnetic systems", *Intern. Conf. on Superconductivity and Magnetism, 29 April - 4 May 2012, Istanbul, Turkey.*

5. A.L. Kuzemsky, "Fundamental Principles of Theoretical Physics and Concepts of Quantum Protectorate and Emergence", *XLVIII All-Russian Conf. on Problems in Particle Physics, Plasma Physics, Condensed Matter, and Optoelectronics, May 15-18, 2012, RUDN, Moscow, Book of Abstracts, p.11-14.*

6. A.L. Kuzemsky,"To the Problem of the Intrinsic Magnetism in Carbon-Based Systems", *Intern. Conf. "DUBNA-NANO12", July 09-14, 2012, JINR, Dubna, Book of Abstracts, p.72.*

7. N.M. Plakida, "Microscopic theory of the magnetic resonance mode", *Eur. Conf. "Physics of Magnetism" - PM-11, 27.06 - 01.07.2011, Poznan, Poland.*

8. N.M. Plakida, "Microscopic theory of spin excitations in cuprates", *Moscow Intern. Symp. on Magnetism, MISM-11, 21.08 - 25.08.2011, Moscow, Russia.*

9. N.M. Plakida, "Spin excitations and mechanisms of superconductivity in cuprates", *4th Intern. Conf. "Fundamental Problems of High-temperature Superconductivity", 03.10 - 07.10.2011, Zvenigorod, Russia.*

10. N.M. Plakida, "Spin excitations and mechanisms of superconductivity in cuprates", *Intern. Workshop "Bogoliubov's Readings", 12.10 - 15.10.2011, Dubna, Russia.*

11. N.M. Plakida, "Spin excitations and mechanisms of superconductivity in cuprates", *in Proceedings of the 4-th Intern. Conf. on Fundamental Problems of High Temperature Superconductivity, Lebedev Physical Institute RAN, Moscow, 2011, pp. 24-27.*

12. N.M. Plakida, "Theory of high-temperature superconductivity in cuprates", *XII Conf. of Young Scientists, "Problem of solid state physics and high-pressure", Sochi, 2012, http://www.hppi.troitsk.ru/meetings/school/XII-2012/xii-sch.htm.*

13. I. Rahmonov, "Mathematical modeling of intrinsic Josephson junctions with capacitive and inductive couplings," *International Conference Dubna-Nano 2012, BLTP JINR, Dubna, Russia, July 9-14, 2012.*

14. D. Sornette, V.I. Yukalov, "Quantum decision theory", *Symposium on Science of Large-Scale Systems, 2012, NASA, Moffett Field, USA.*

15. N.S. Tonchev, J.G. Brankov, "Bounds on the Bogoliubov-Duhamel inner product with applications in phase transitions and quantum information", *Intern. Workshop "Bogoliubov's Readings", 12.10 - 15.10.2011, Dubna, Russia.*

16. V.I. Yukalov, E.P. Yukalova, "Critical region of Bose-condensation transition in mean-field approximation", *Intern. Workshop on Laser Physics, 2012, Calgary University, Calgary, Canada.*